2010

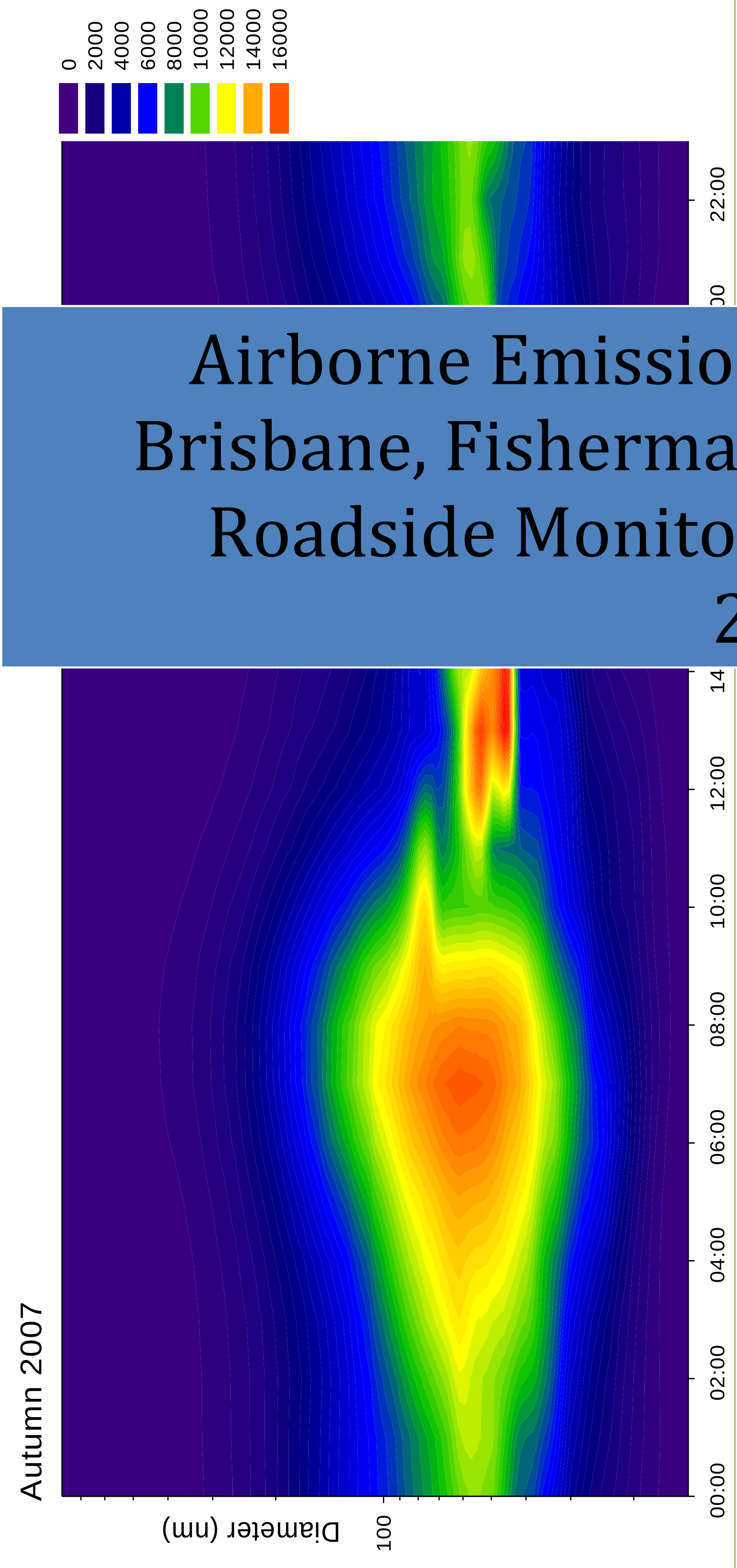

Airborne Emissions- Port of Brisbane, Fisherman Islands - Roadside Monitoring Study 2006-2008

Morawska and Johnson

International Laboratory for Air Quality and Health - Queensland University of Technology

22nd March, 2010

Airborne Emissions- Port of Brisbane, Fisherman Islands

Roadside Monitoring Study 2006-2008

Presented to the Port of Brisbane Corporation

Professor Lidia Morawska
Dr Graham Johnson
International Laboratory for Air Quality and Health
Queensland University of Technology

March 2010

EXECUTIVE SUMMARY

This report presents an overview of the data collected in the Airborne Emissions-Port of Brisbane, Fisherman Islands Roadside Monitoring Study 2006-2008. The study aims to improve our knowledge of the current airborne pollutant emissions in the Fisherman Islands precinct to provide a baseline from which predictions can be made concerning the impact of future growth of the port and the resulting emissions in the precinct. The study therefore provides detailed information on airborne pollutant concentrations near the port, focussing on the land transport access corridor for the Fisherman Islands precinct, a major source of airborne pollutants associated with port activity. It examines the relationships between airborne pollutant concentrations and port road traffic intensity to provide a basis for predictions of future concentrations in the corridor as the intensity of transport activity changes.

To achieve this, airborne pollutants, including particle size distribution, particle number concentration, fine particle mass concentration, sulphur dioxide, and oxides of nitrogen, as well as meteorological variables including wind speed and direction were measured for a total of sixteen weeks in eight seasonal campaigns spanning a two year period from January 2006 to February 2008. The monitoring was conducted from a trailer located between Port Drive, and the Railway line, at the southern tip of Fisherman Islands, immediately north of Captain Bishop Bridge.

The report presents the seasonal and diurnal pattern of pollutant concentration and particle size distribution and examines the dependence of these on wind direction, and land utilisation. The effect of varying traffic intensity on the concentrations of each of the pollutants is examined and the relationships between them are described mathematically. The degree to which the sampling periods were representative of typical seasonal meteorological conditions in the area is also examined.

The analysis reveals a strong dependence of pollutant concentrations on land use, evident in strong relationships between wind direction and concentration. Four distinct source-sectors were identified:

- The Clean Air source-sector ranging from northeast through to southeast and influenced by the marine environment and Southern Moreton Bay Islands. This source-sector is also influenced by rail traffic emissions.

- The Residential source-sector ranging from southeast through to the south and taking in the residential community of Wynnum North and beyond. This source-sector also receives some influence from road traffic emissions from Port Drive.

- The Lower Brisbane Industrial source-sector, ranging from south through to west and taking in all of the Caltex and much of the BP oil refineries and strongly influenced by road traffic emissions from Port Drive.

- The Port Activities source-sector ranging from west through to northeast and taking in the industrial areas of Port of Brisbane's Fisherman Islands complex and strongly influenced by road traffic emissions from Port Drive and susceptible to influences from the BP Oil refinery, Luggage Point area and Brisbane Airport.

There was no indication of a prominent source of fine dust particles in the Port Activities source-sector. More of this material was associated with the Lower Brisbane Industrial than the Port Activities source-sector. Road traffic on Port Drive, common to both the Lower Brisbane Industrial and Port Activities source-sectors was the dominant source in both of those source-sectors.

The concentration was highest in the Lower Brisbane Industrial and Port Activities source-sectors for all pollutants measured. In the case of sulphur dioxide and to a lesser extent nitrogen dioxide the highest concentrations were associated with the Brisbane Industrial and Port Activities source-sectors. For particle number concentration and fine particle concentrations however, the Clean Air and Residential source-sectors made significant contributions at the measuring site. The strongest contribution on average came from the Lower Brisbane Industrial source-sector for all but sulphur dioxide concentration, while for sulphur dioxide the concentrations associated Port Activities and Lower Brisbane Industrial source-sectors were similar.

The concentrations of oxides of nitrogen, fine particles, sulphur dioxide and particle number concentration measured in air which had passed over the Port Activities source-sector were not significantly elevated in comparison to those measured in air which had passed over the Lower Brisbane Industrial source-sector. The traffic on Port Drive was the dominant source of all of the pollutants measured at the monitoring site.

Contents

1 Introduction

Given the increased growth of the Port of Brisbane Corporation (PBC), and ongoing developments within the port expansion area, assessments of airborne emissions including particulate and gaseous emissions are desirable if future needs for appropriate control measures are to be anticipated so that high standards of air quality continue to be achieved. To this end, the study aims to improve our knowledge of the current airborne pollutant emissions in the Fisherman Islands precinct. This will provide a baseline from which predictions can be made concerning the impact of future growth of the port and the resulting emissions in the precinct.

The study provides detailed information on airborne pollutant concentrations near the port, focussing on the land transport access corridor for the Fisherman Islands precinct, a major source of airborne pollutants associated with port activity. The study examines the relationships between airborne pollutant concentrations and port road traffic intensity to provide a basis for predictions of future concentrations in the corridor as the intensity of transport activity changes.

Airborne pollutants, including particle size distribution, particle number concentration, $PM_{2.5}$, SO_2, and NO_x as well as meteorological variables including wind speed and direction were measured for a total of 16 weeks in eight campaigns timed as per Table 1.

Table 1: Campaign dates

Campaign Dates	***Dates***
1 Autumn 2006	15/05/2006-31/05/2006
2 Winter 2006	18/08/2006-04/09/2006
3 Spring 2006	31/10/2006-15/11/2006
4 Summer 2006/7	11/01/2007-30/01/2007
5 Autumn 2007	23/05/2007-01/06/2007
6 Winter 2007	20/08/2007-12/09/2007
7 Spring 2007	02/11/2007-25/11/2007
8 Summer 2007/8	31/01/2008-21/02/2008

The monitoring was conducted from a trailer designed for the purpose, located at the Southern tip of Fisherman Islands between Port Drive, and the Railway line. The pollutant and meteorological measurements were performed by the International Laboratory for Air Quality and Health (ILAQH) Queensland University of Technology in collaboration with The Port of Brisbane Corporation (PBC). Road and rail traffic data were provided by PBC.

2 Approach

The measurements conducted during each of the campaigns included:

- Particle sub-micrometer size distribution
- Particle number concentration (Cn) for particles larger than 14 nm
- $PM_{2.5}$ particulate mass concentration
- NO_x and SO_2 concentrations
- Meteorological conditions
- Road and rail traffic intensity (data provided by Port of Brisbane Corporation)

The following instrumentation was mounted in the monitoring trailer adjacent to the access road inside the secure perimeter of the port area.

- R&P TEOM with $PM_{2.5}$ inlet.
- Scanning mobility Particle Sizer (SMPS) (TSI SMPS 3934)
- Ambient NO_x analyser (Ecotech EC9841A NO_x analyser)
- Ambient SO_2 analyser (Monitor Labs 9850)
- Weather Station (Monitor Instruments)

3 Measurement and Analytical Methods

3.1 Location of Sampling Site

The Port Drive site (shown in Figure 1) is situated near the southern end of Fisherman Islands on the western side of Port Drive, between that road and the railway line. Port Drive and the railway line follow a straight almost north-south path near the site. The sampling was conducted eight metres east of the centre line of Port Drive twelve metres west of the centre of the railway line and three metres above the ground surface.

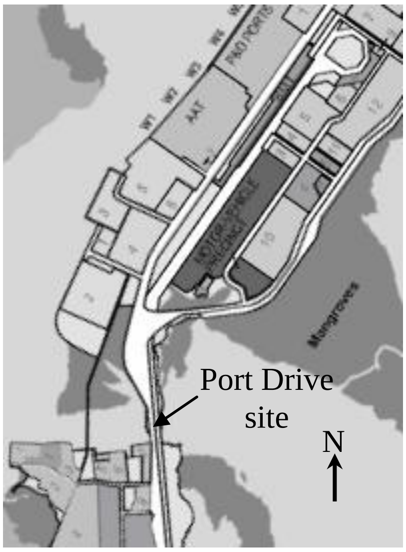

Figure 1 Location of the Port Drive site

3.2 Instrumentation

The particle number concentration for particles larger than 0.010 µm was measured continuously using a TSI 3934 Scanning Mobility Particle Sizer (SMPS). The SMPS consists of a TSI 3071A electrostatic classifier (EC) and a TSI 3010 condensation particle counter (CPC). The EC classifies particles according to size while the CPC counts the number of particles in each size classification. An interfacing computer controls the process of measurement and stores the data supplied by the counter.

The mass concentration of particulate matter with aerodynamic diameter smaller than 2.5 µm, known as $PM_{2.5}$, was measured continuously using a Tapered Element Oscillating Microbalance (TEOM) (Rupprecht & Pretashnick, TEOM 1400a) fitted with a 2.5 µm aerodynamic diameter cut-point cyclone. The NO_2 concentration was measured using an Ecotech 9841 NO_x analyser. The SO_2 concentration was measured using an Ecotech 9850 SO_2 analyser.

All instruments were operated from a monitoring trailer which was also fitted with a Monitor Sensors MS1 portable weather station. The weather station monitored wind direction and speed as well as a range of other meteorological variables including temperature, relative humidity, atmospheric pressure and solar radiation intensity.

Road and rail traffic past the site were monitored continuously throughout each of the four measurement campaigns. This data was provided by the Port of Brisbane Corporation.

SMPS calibration consisted of flow calibration of the sheath and aerosol flow rates using a bubble flow meter and sizing verification using 102nm NIST traceable PSL shears. TEOM mass flow controllers were verified by comparison against a bubble flow meter at the standard operational flow rates. The NO_x and SO_2 analysers were serviced and calibrated by certified calibration service prior to the campaigns and regular zero checks were performed using a zero air source.

3.3 Monitoring and Sampling Procedures

The SMPS, CPC, NO_x, SO_2, TEOM and weather station were operated continuously, recording concentration and wind direction. The size distribution and concentration data were therefore able to be classified according to wind direction to obtain a measure of the angular distribution of the particle size and concentration at the site with respect to wind direction.

3.4 Data Analysis

3.4.1 Data Timing and Synchronisation

The weather station, CPC, SO_2, NO_x and TEOM systems operate independently, providing time series data at regular intervals of less than one hour. In order to facilitate data analysis, the data from each instrument was translated to a common time-base by interpolating between adjacent data points of each instruments time series to establish the concentration at a common time. This process results in synchronous data on a common hourly time base.

3.4.2 Statistics

Comparisons were made using parametric or non-parametric statistical methods as appropriate. Average, standard deviation and maximum values are reported here. The 0.05 level of significance was used throughout and all reported p-values are two-sided unless otherwise stated.

4 Results

The following results are presented below:

- Time series data for each of the eight campaigns
  - Campaign specific time series concentration data for total particle number concentration, $PM_{2.5}$, NO_x, SO_2 and meteorological data including local wind speed and direction.
    - Comparison with relevant National Environment Protection Measure (NEPM) and Advisory NEPM (ANEPM) thresholds.
  - Campaign specific time series data for particle size distribution.
- Seasonal variations
  - Comparison of the corresponding seasonal concentration averages and standard deviations in both years of the study.
  - Average particle size distributions associated with the seasons over the whole study.
- Wind direction influence on concentration.
  - Compass sector specific particle and gas concentration data showing how concentration depends on wind direction
  - Compass sector specific particle number size distribution
  - The relationship between traffic intensity and roadside concentration for winds from Port Drive, predicting traffic intensity where NEPM and ANEPM thresholds may be reached.
- Assessment of the extent to which the wind conditions during each two week measurement period are representative of historical seasonal behaviour.

The results therefore present a comprehensive overview of the seasonal and diurnal pattern of airborne pollutant concentrations and particle size distribution, as well as the simultaneous temporal variation of road and rail traffic intensity and the simultaneous patterns of wind direction and wind speed change.

4.1 Time series data for each of the eight campaigns

4.1.1 Campaign specific time series pollutant concentrations

The times series concentration data in the first and second campaign years for each season are presented in Figure 2 to Figure 9 along with the relevant NEPM and ANEPM thresholds. All variables except $PM_{2.5}$ are presented as time centred one hour average data, which with the exception of the rail traffic intensity and wind direction data are represented by an interpolating line connecting of the hourly data points. Because rail traffic typically passed only infrequently, this data is instead represented by discrete bars representing the hourly average values. Wind direction data are also presented as discrete hourly values to avoid a messy data presentation with line discontinuities where data passes over the 0° (360°) pole. $PM_{2.5}$ data are presented as hourly values of the sliding 24 hour average to ensure a reasonable signal to noise ratio.

Intervals of missing concentration data are visible in the time series. Nevertheless a total of 14 days of measurement were recorded for size distributions and all concentration variables in all except one campaign, in which only 10 days were recorded. These interruptions correspond to instrument, power, computer, or data communication issues and to intervals where the data was considered suspect due to water condensation in the sampling inlet lines. Traffic data was supplied in a different format during winter 2006 and spring 2006 and while the data was more comprehensive, the total vehicle count does not appear to have been assessed in the same way as during the remaining campaigns. In the former peak traffic intensities of only 400-500 per hour are regularly achieved whereas the data for the remaining campaigns show intensity peaks regularly in excess of 1000 per hour.

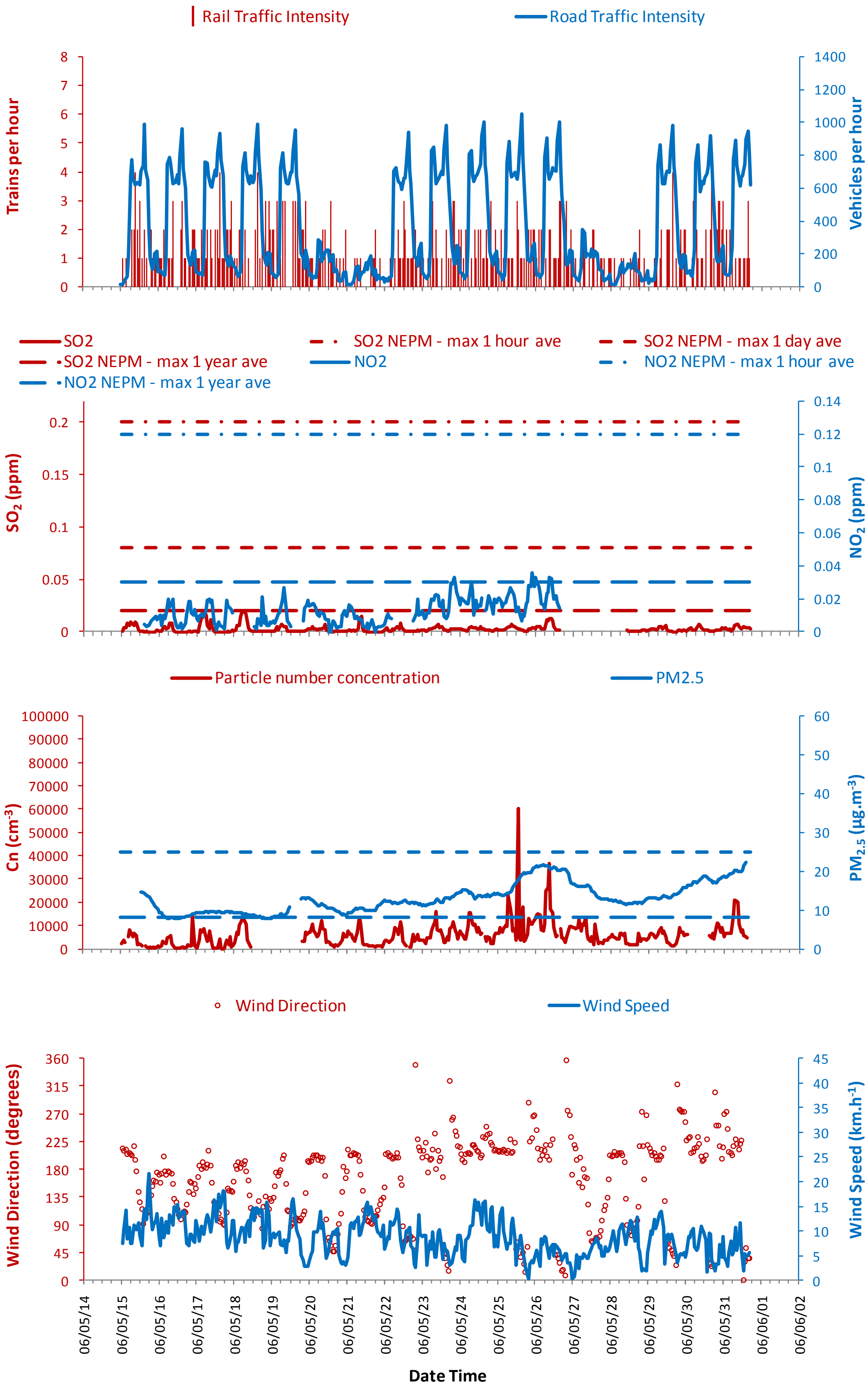

Figure 2: Hourly rail and road traffic intensities; SO_2, NO_x, Cn, and $PM_{2.5}$ concentrations; and wind direction and speed time series data - Autumn 2006. ($PM_{2.5}$ data is 24 hour).

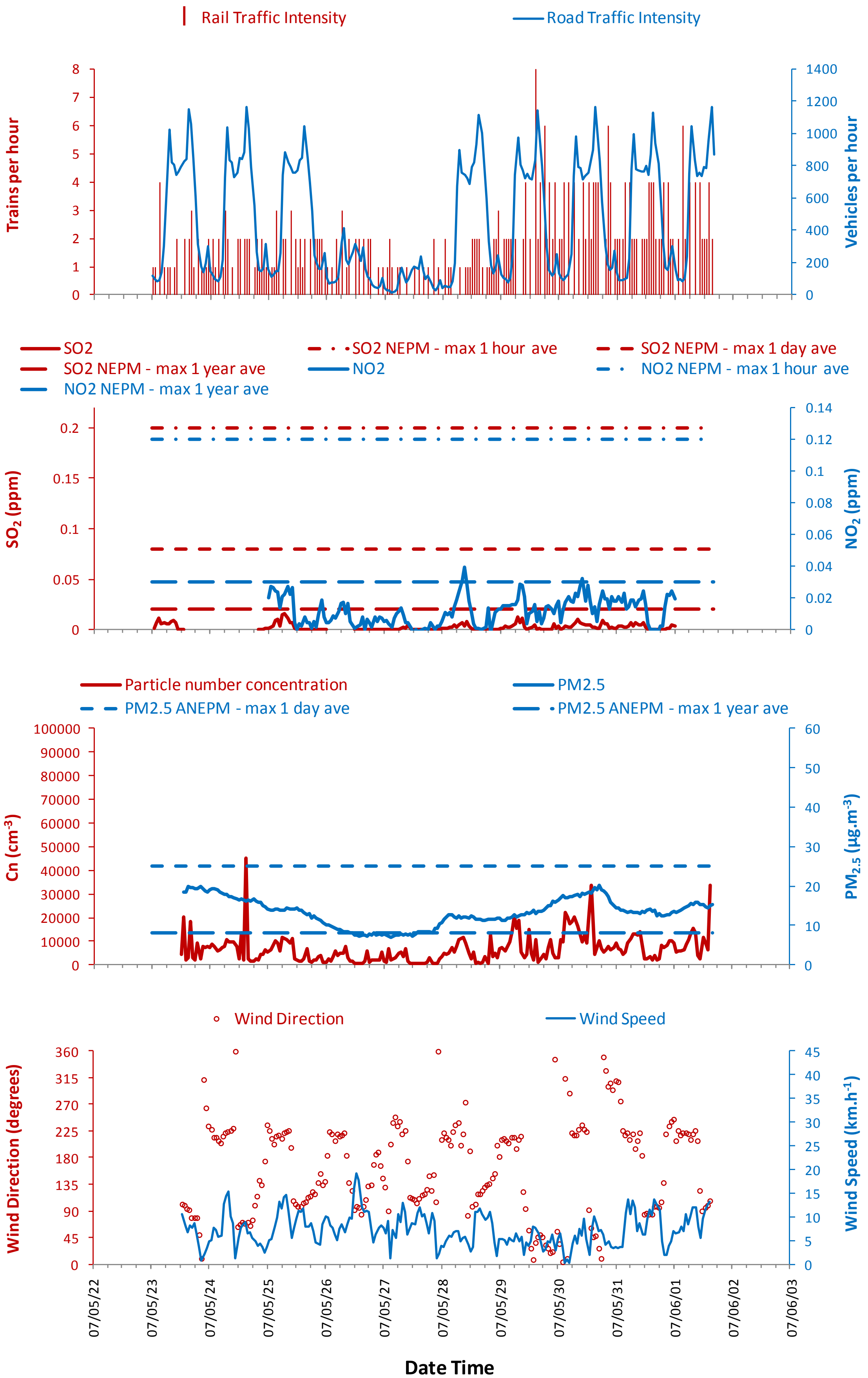

Figure 3: Hourly rail and road traffic intensities; SO_2, NO_x, Cn, and $PM_{2.5}$ concentrations; and wind direction and speed time series data - Autumn 2007. ($PM_{2.5}$ data is 24 hour).

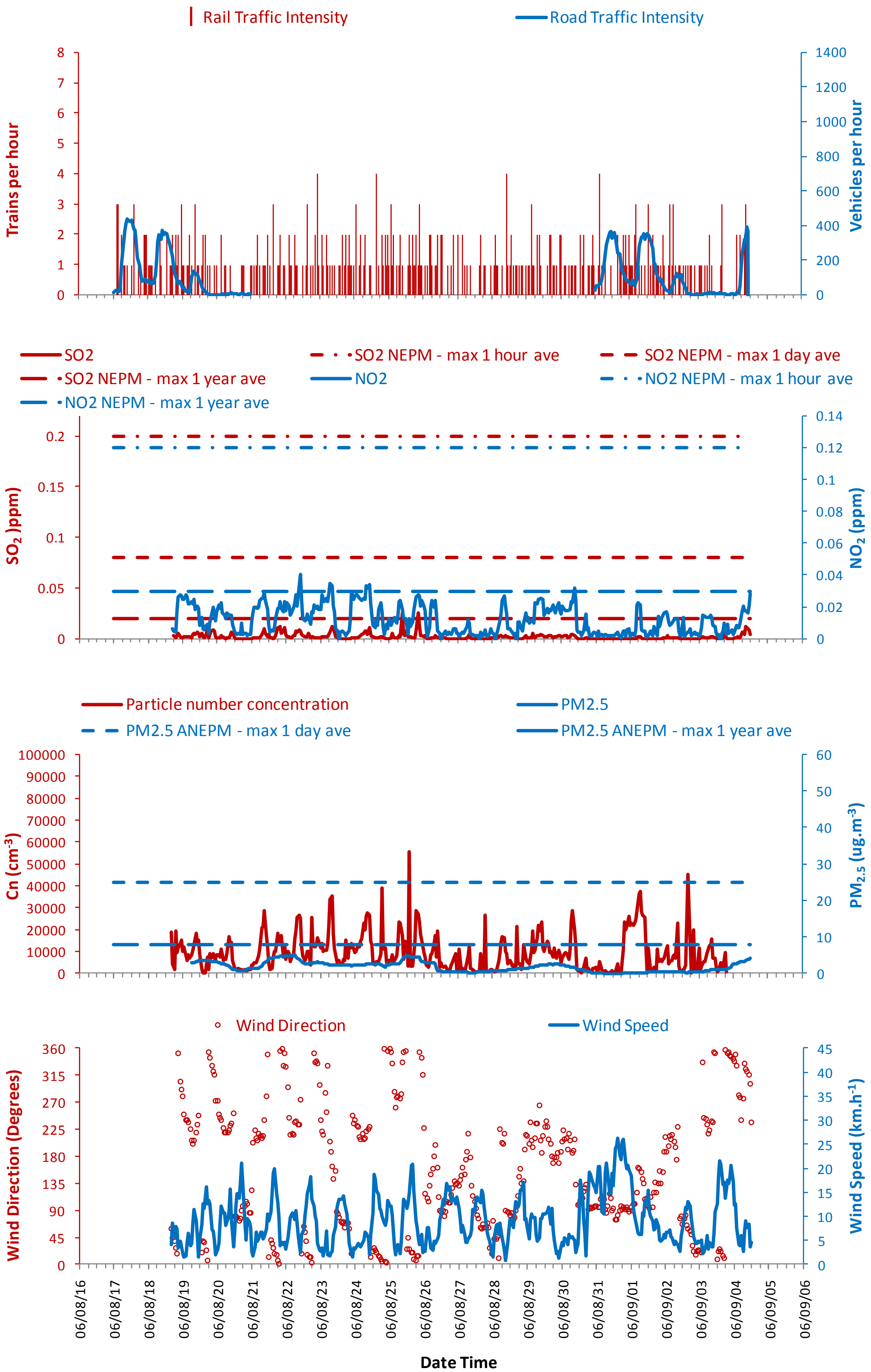

Figure 4: Hourly rail and road traffic intensities; SO_2, NO_x, Cn, and $PM_{2.5}$ concentrations; and wind direction and speed time series data - Winter 2006. ($PM_{2.5}$ data is 24 hour).

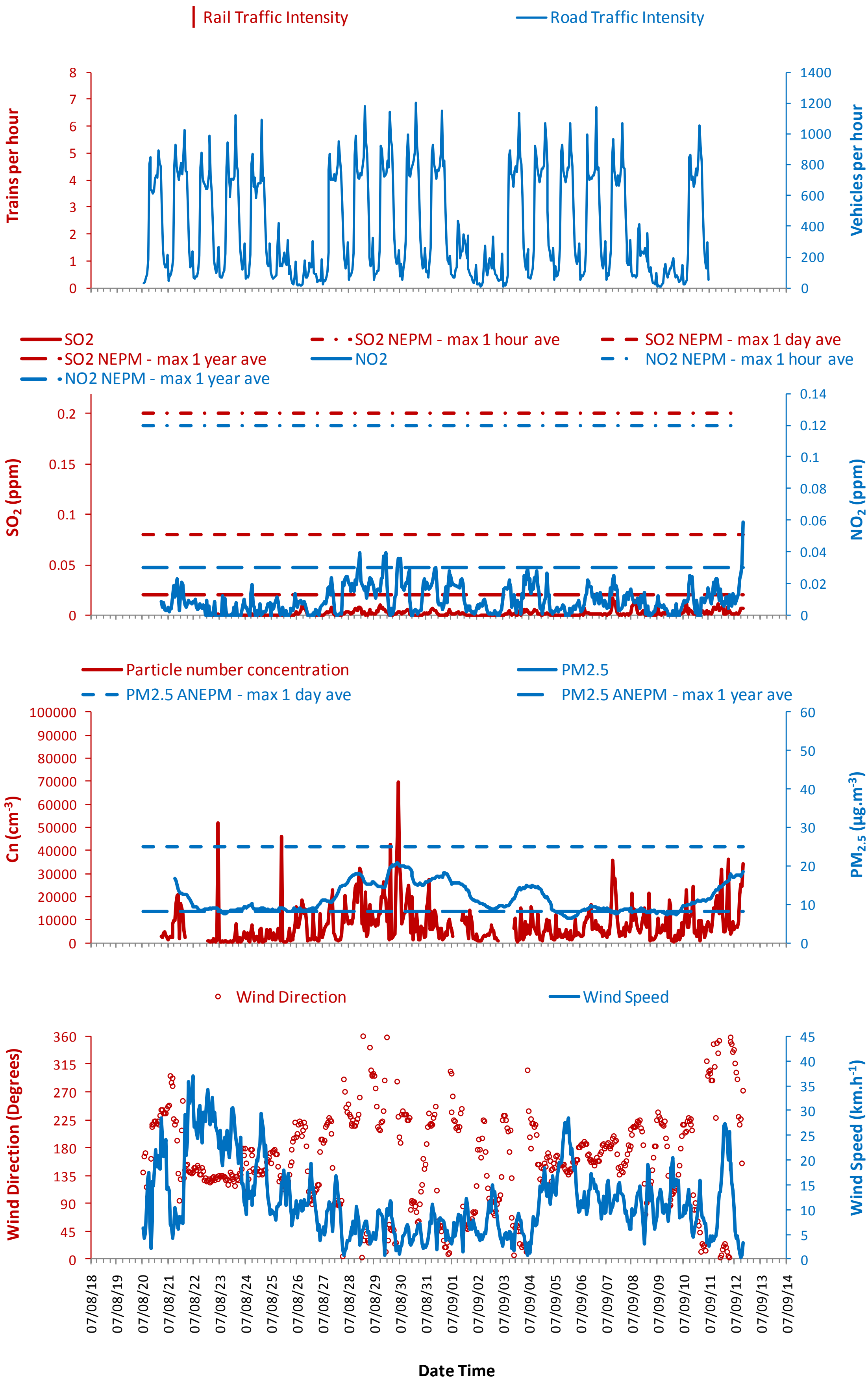

Figure 5: Hourly rail and road traffic intensities; SO_2, NO_x, Cn, and $PM_{2.5}$ concentrations; and wind direction and speed time series data - Winter 2007. ($PM_{2.5}$ data is 24 hour).

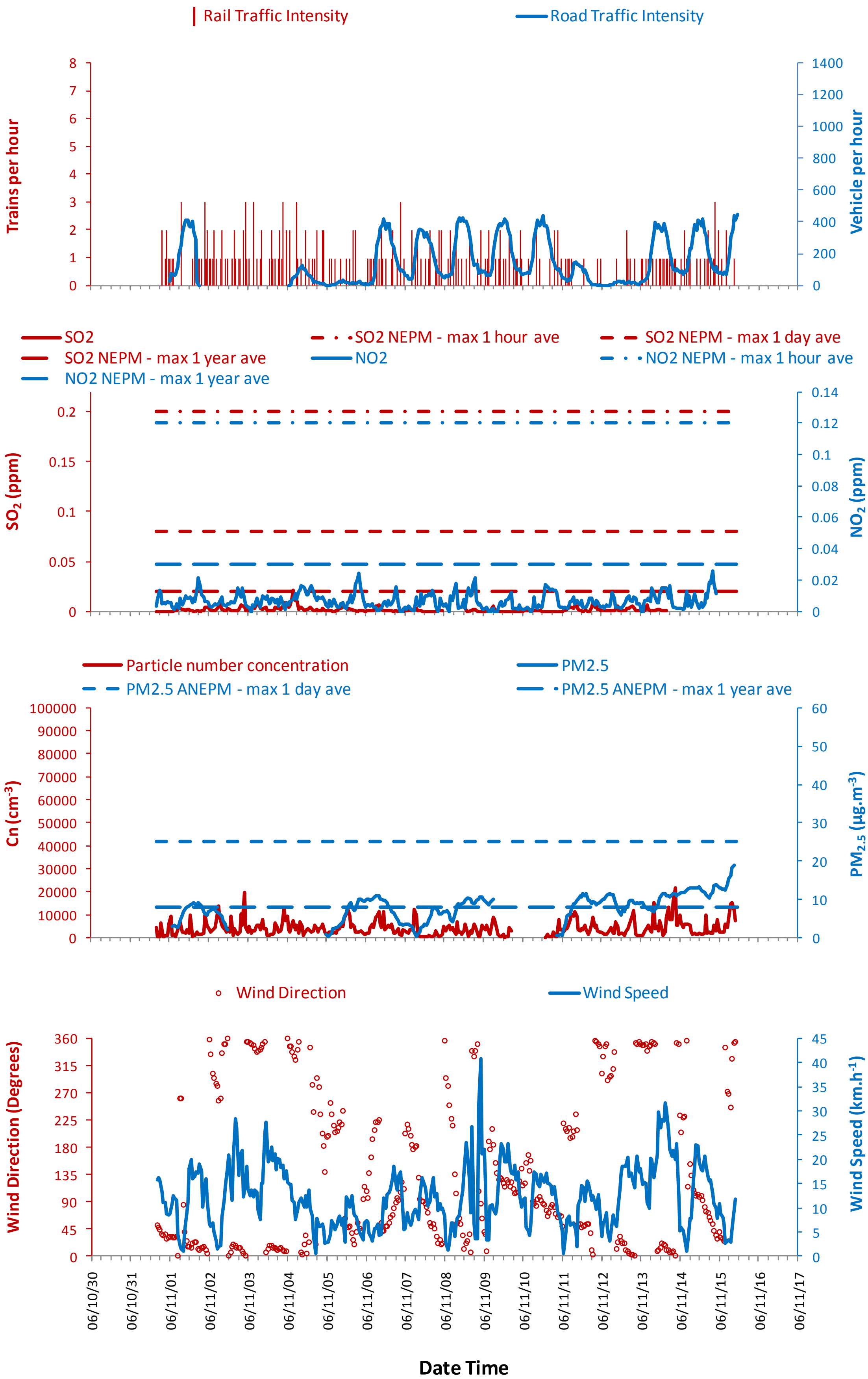

Figure 6: Hourly rail and road traffic intensities; SO_2, NO_x, Cn, and $PM_{2.5}$ concentrations; and wind direction and speed time series data - Spring 2006. ($PM_{2.5}$ data is 24 hour).

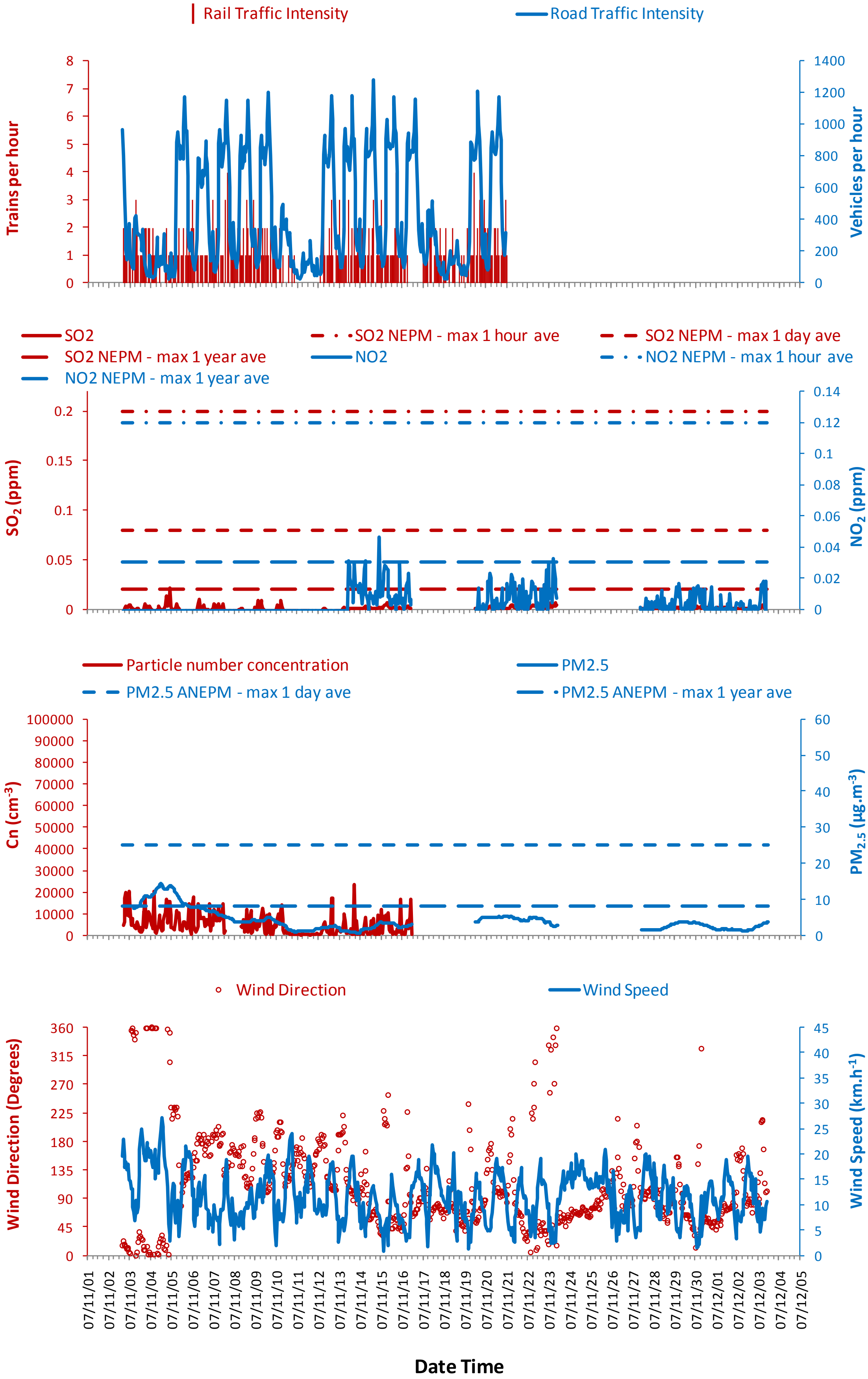

Figure 7: Hourly rail and road traffic intensities; SO_2, NO_x, Cn, and $PM_{2.5}$ concentrations; and wind direction and speed time series data - Spring 2007. ($PM_{2.5}$ data is 24 hour).

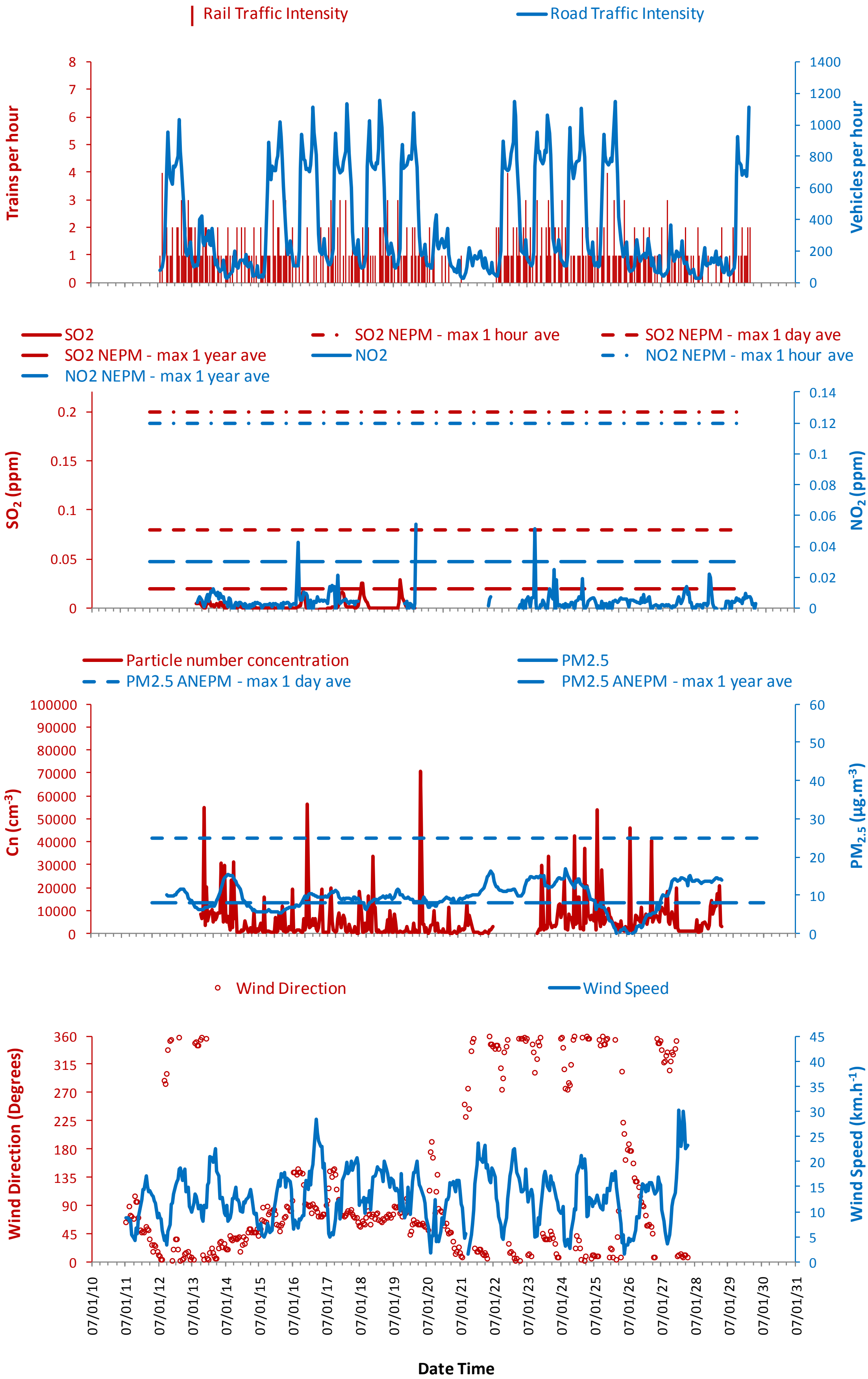

Figure 8: Hourly rail and road traffic intensities; SO_2, NO_x, Cn, and $PM_{2.5}$ concentrations; and wind direction and speed time series data - Summer 2006-7. ($PM_{2.5}$ data is 24 hour).

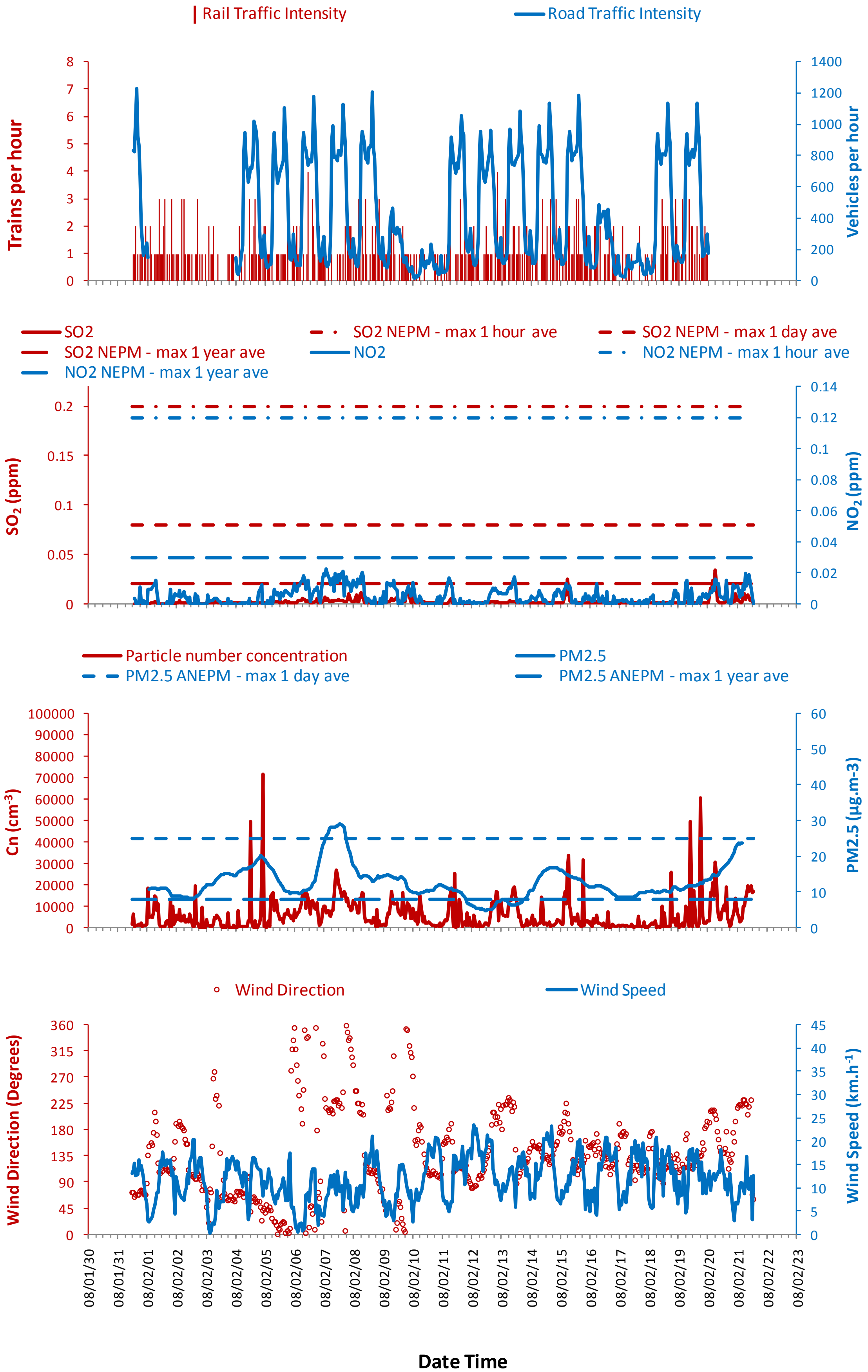

Figure 9: Hourly rail and road traffic intensities; SO_2, NO_x, Cn, and $PM_{2.5}$ concentrations; and wind direction and speed time series data - Summer 2007-8. ($PM_{2.5}$ data is 24 hour).

The road traffic shows a well defined weekly cycle characterised by distinct work-day (Monday through Friday) and weekend (Saturday and Sunday) intraday patterns. The work-day pattern has high intensity between 6:00 AM and 6:00 PM with peaks at 7:00 AM 3:00 PM. Intensity outside of this period is low. The intensity is generally much lower on weekends.

The one hour average SO_2 concentration did not exceed the NEPM maximum for a one hour average at any point during the measurements. Similarly the one hour average NO_2 concentration did not exceed the NEPM maximum for a one hour average at any point during the measurements.

The 24 hour average $PM_{2.5}$ concentration exceeded the ANEPM maximum for one day averages on a single occasion. This occurred on 7th February 2008 during light south westerly winds between midnight and 6:00 PM.

The particle number concentration time series data was characterised by a very high degree of variability, due to the close proximity of motor vehicle traffic. Passing motor vehicles present an intense and highly variable source of submicrometer particles. This variation further enhanced by the presence the contrasting very low baseline concentration in the marine environment to the east and diurnal variations in the wind direction will inevitably result in dramatic changes in particle number concentration in such locations. The magnitude of the observed concentration excursions is consistent with this roadside location.

4.1.2 Campaign specific time series for particle size distribution.

The times series particle size distributions for all campaigns are presented in Figure 10 to Figure 17. The size distributions show a predominance of 30-100 nm diameter particles which is typical of traffic emissions.

Particle size distributions produced by a well defined particle generation process (for example fuel combustion) usually have a lognormal size distribution and would therefore be expected to appear as a fairly broad symmetrical peak when presented on a log diameter scale. However plumes from passing motor vehicles are typically present for only a few seconds and the sequential nature of SMPS size distribution measurement, which consists of scanning from the smallest to largest particle sizes over a period of several minutes, often results in the appearance of abrupt excursions in particle concentration at apparently random diameters. Such excursions are evident throughout the size distribution time series graphs. These can also occur when the wind is from other directions for example they can occur when the wind is from the east due to passing trains which produce similar exhaust particle emissions to diesel motor vehicles. Such abrupt and apparently very large concentration events indicate momentary exposure to essentially undiluted exhaust form a passing tuck or train. The frequency of occurrence of such events is highly dependent on the traffic intensity atmospheric stability and wind conditions at the time of measurement.

In these circumstances it is nevertheless possible to build up an average representation of the true size distribution by accumulating scans for many passing vehicles. In doing so it is necessary to choose only those scans which are recorded when the wind is from the direction of the source in which we are interested, for example the road. This approach to the analysis is taken in section *5.3.2 Compass sector specific particle number size distribution*.

Overall the time series size distributions are very consistent with expectation for a location close to a road, carrying a high proportion of diesel vehicles, given diurnal wind changes (sea/land breeze) in conjunction with contrasting polluted and unpolluted source regions as are constituted by the city and Port Drive to the west and the relatively clean marine region to the east.

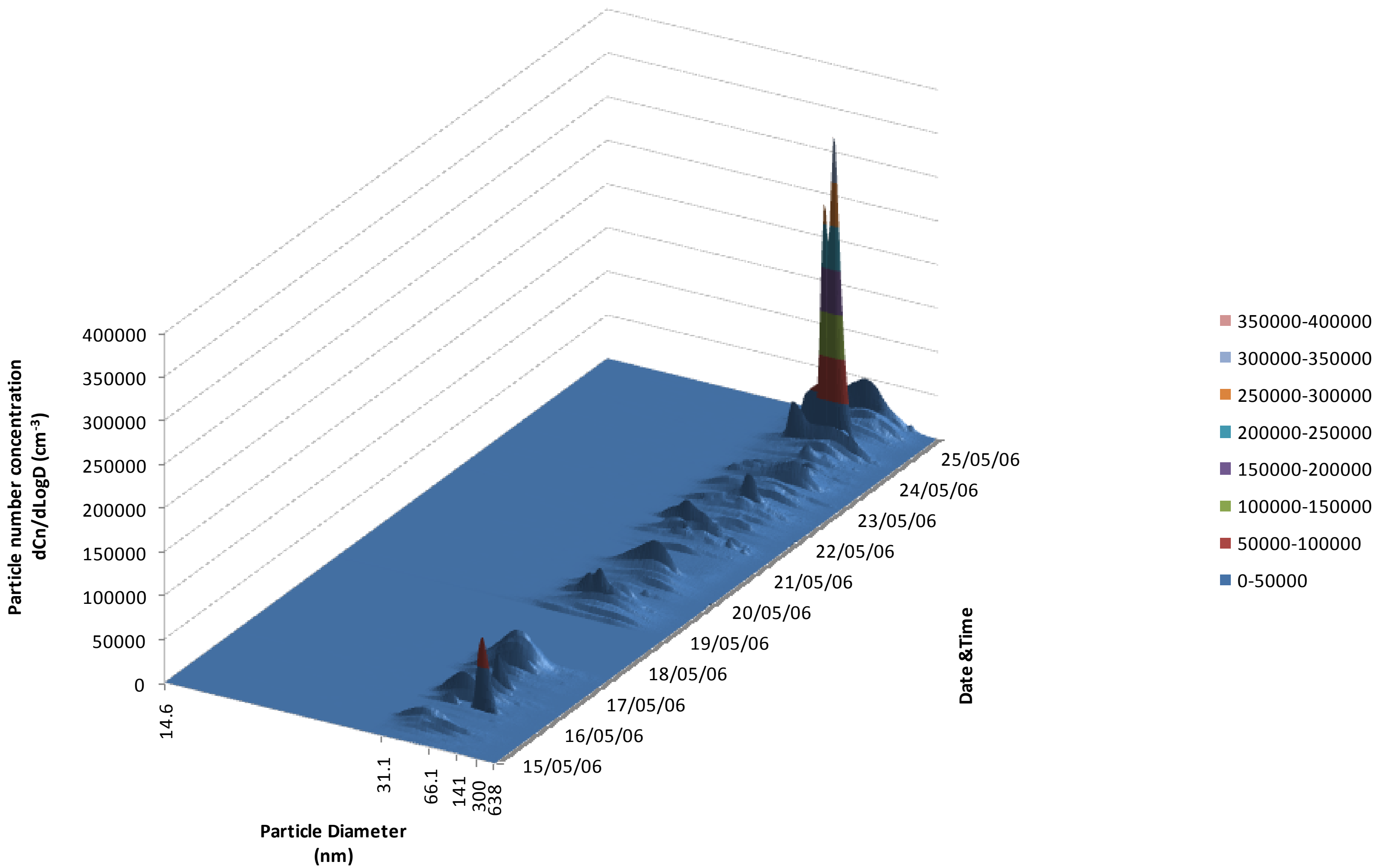

Figure 10: Particle number size distribution time series - Autumn 2006

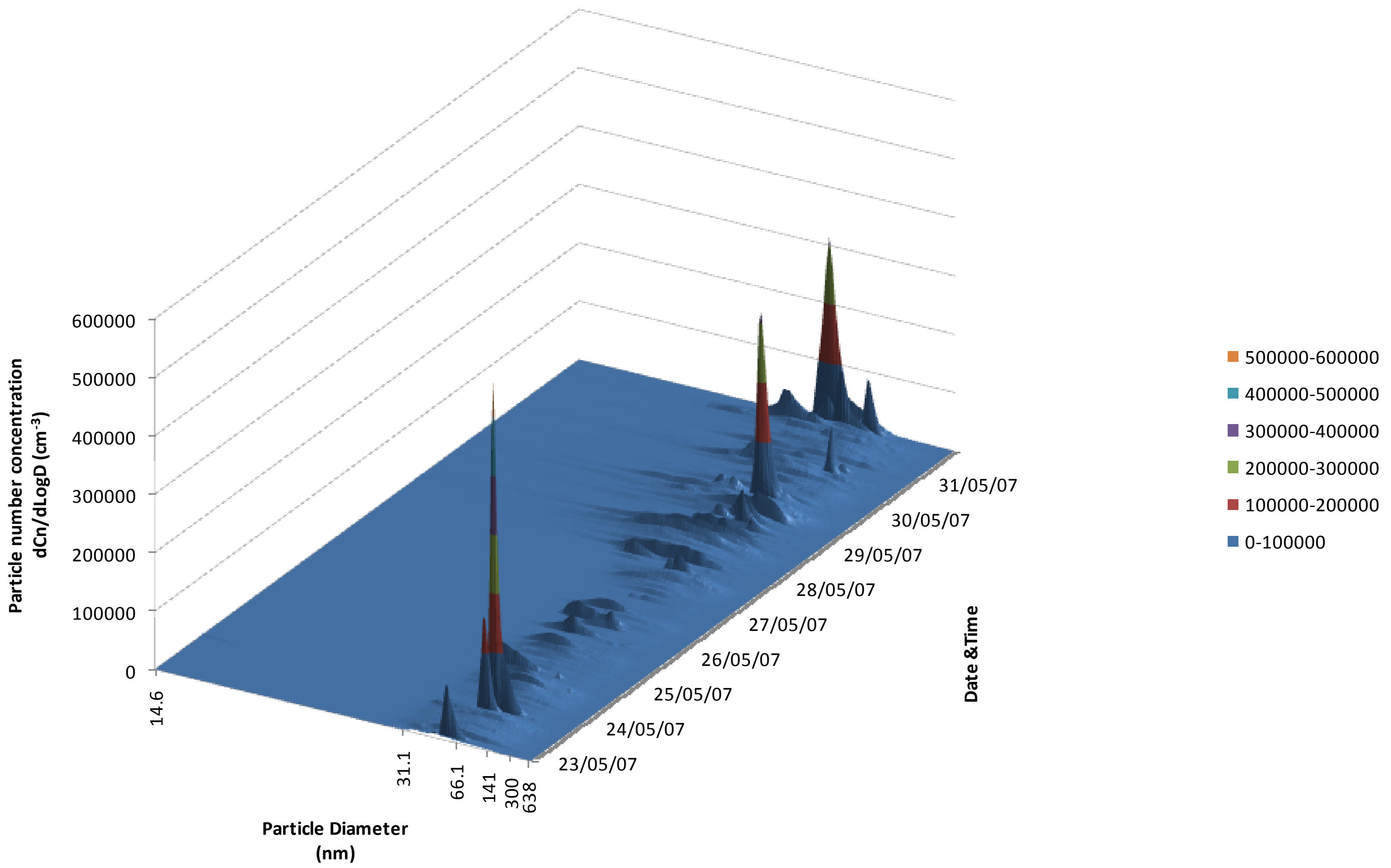

Figure 11: Particle number size distribution time series - Autumn 2007

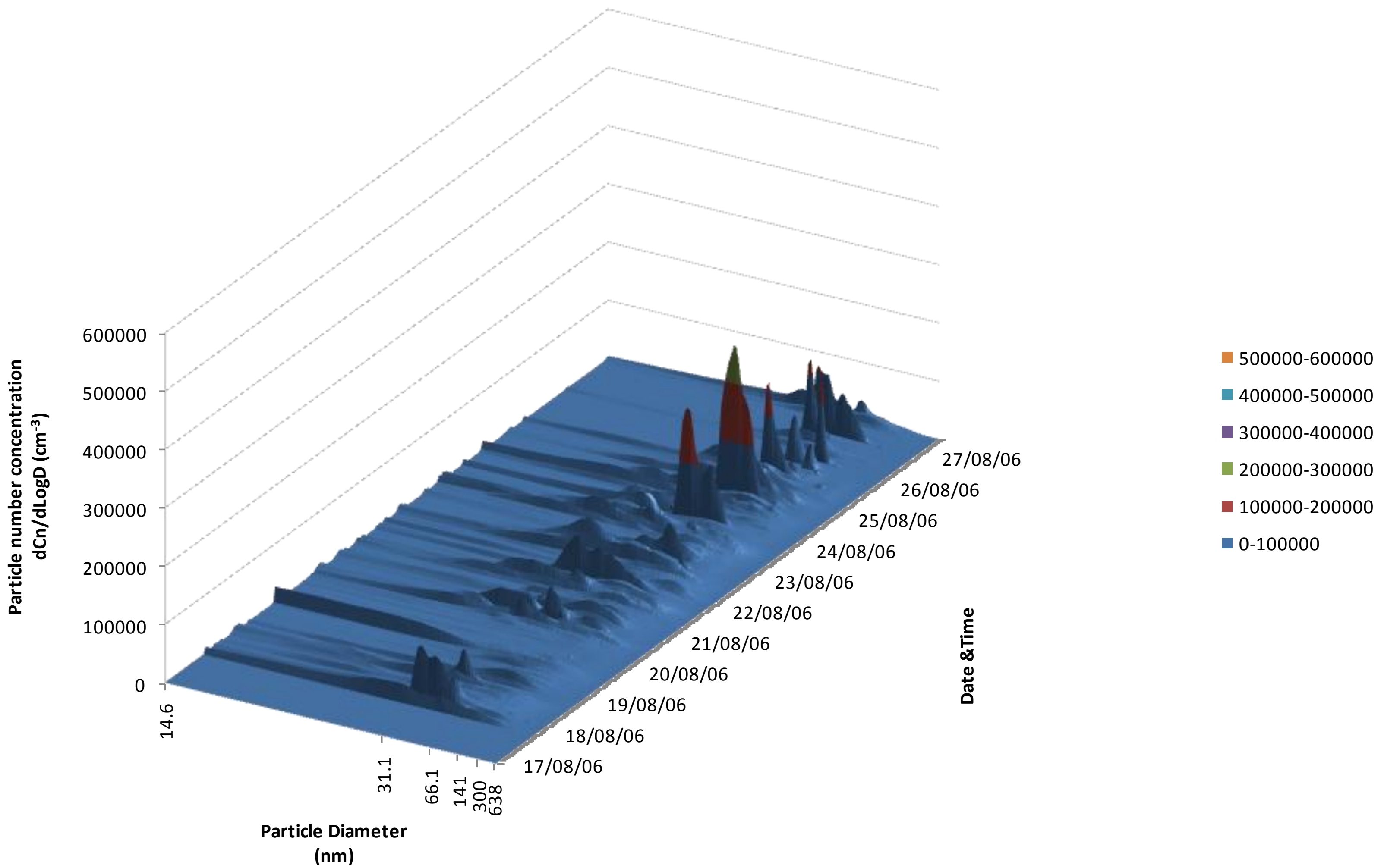

Figure 12: Particle number size distribution time series - Winter 2006

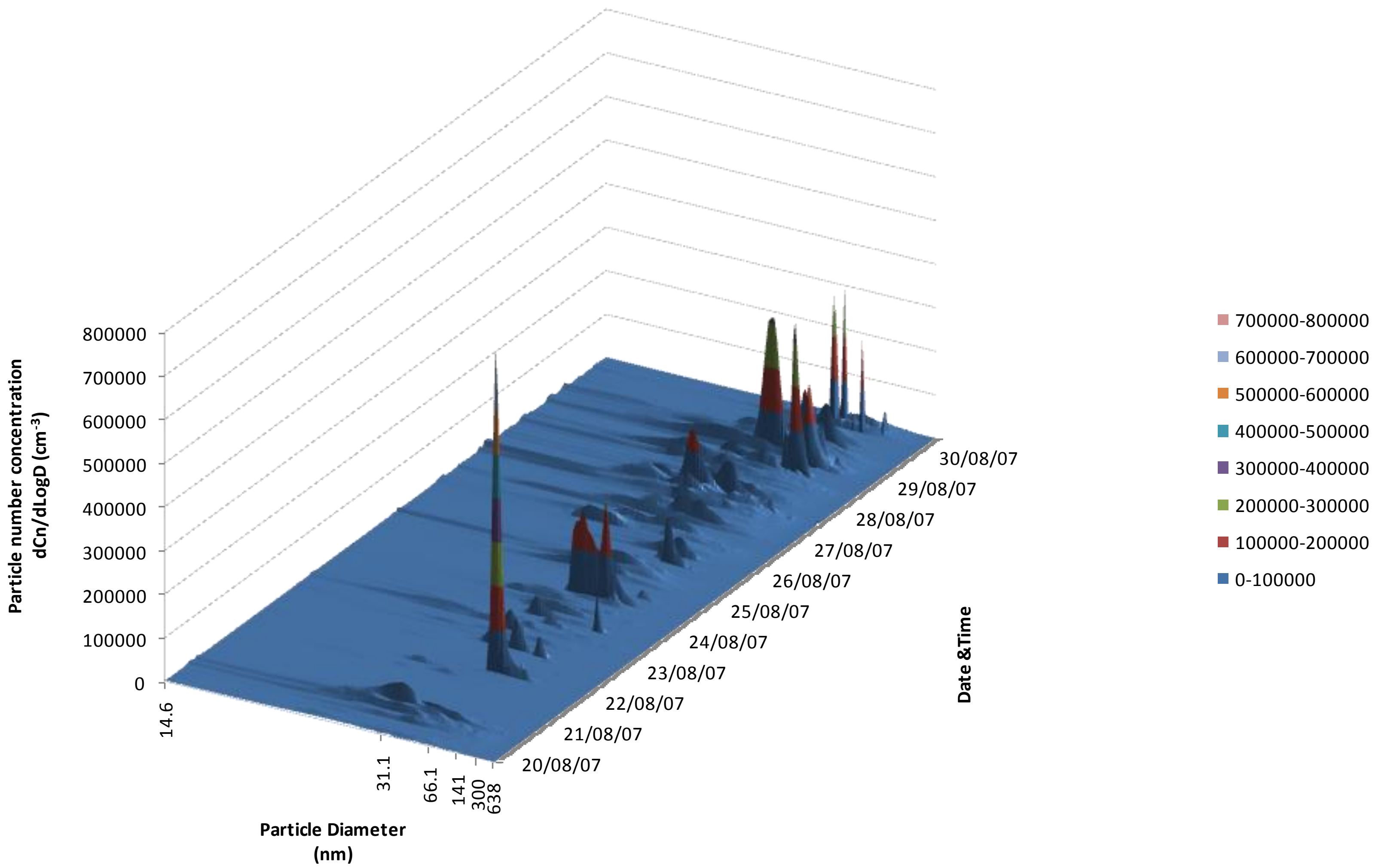

Figure 13: Particle number size distribution time series - Winter 2007

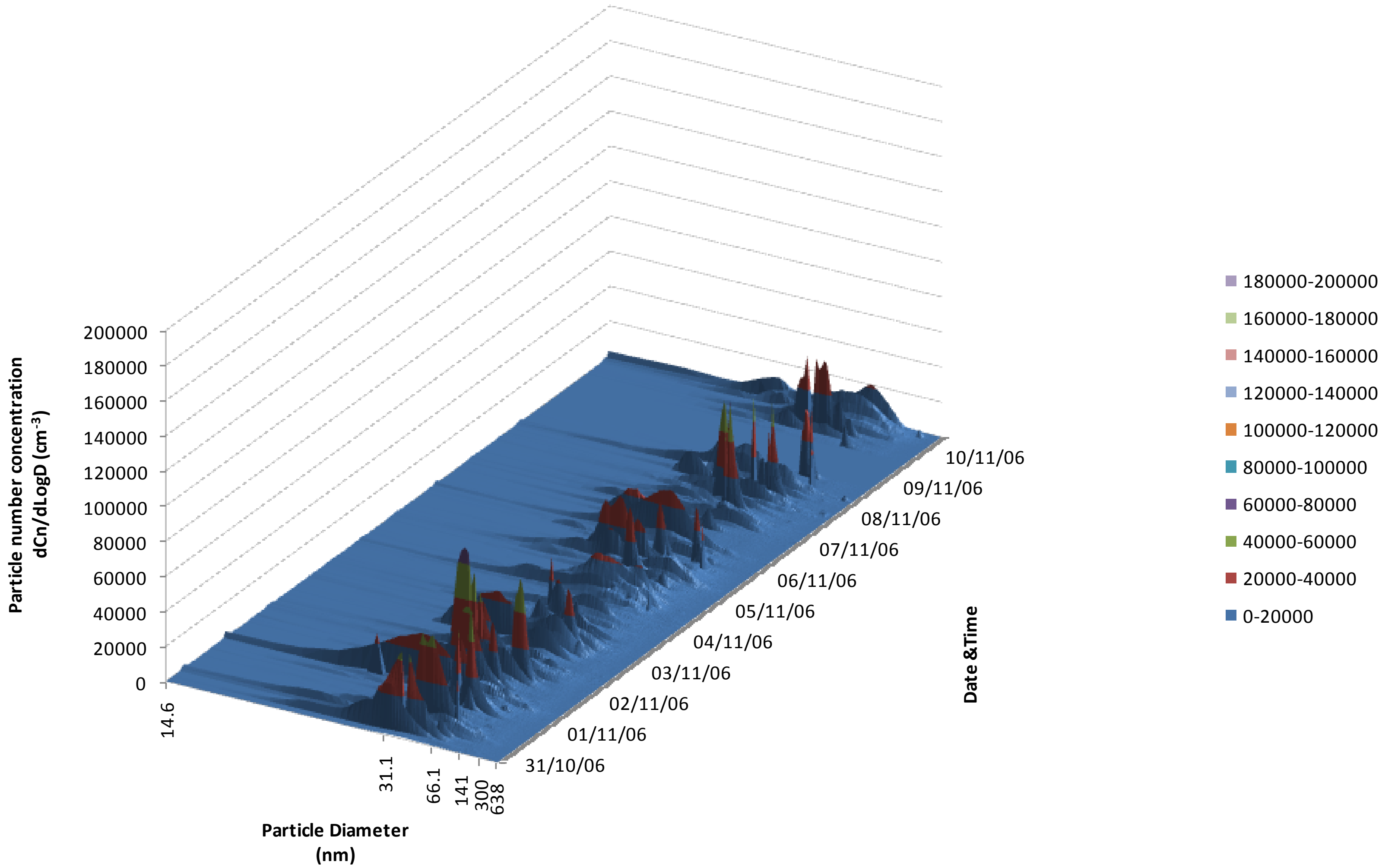

Figure 14: Particle number size distribution time series - Spring 2006

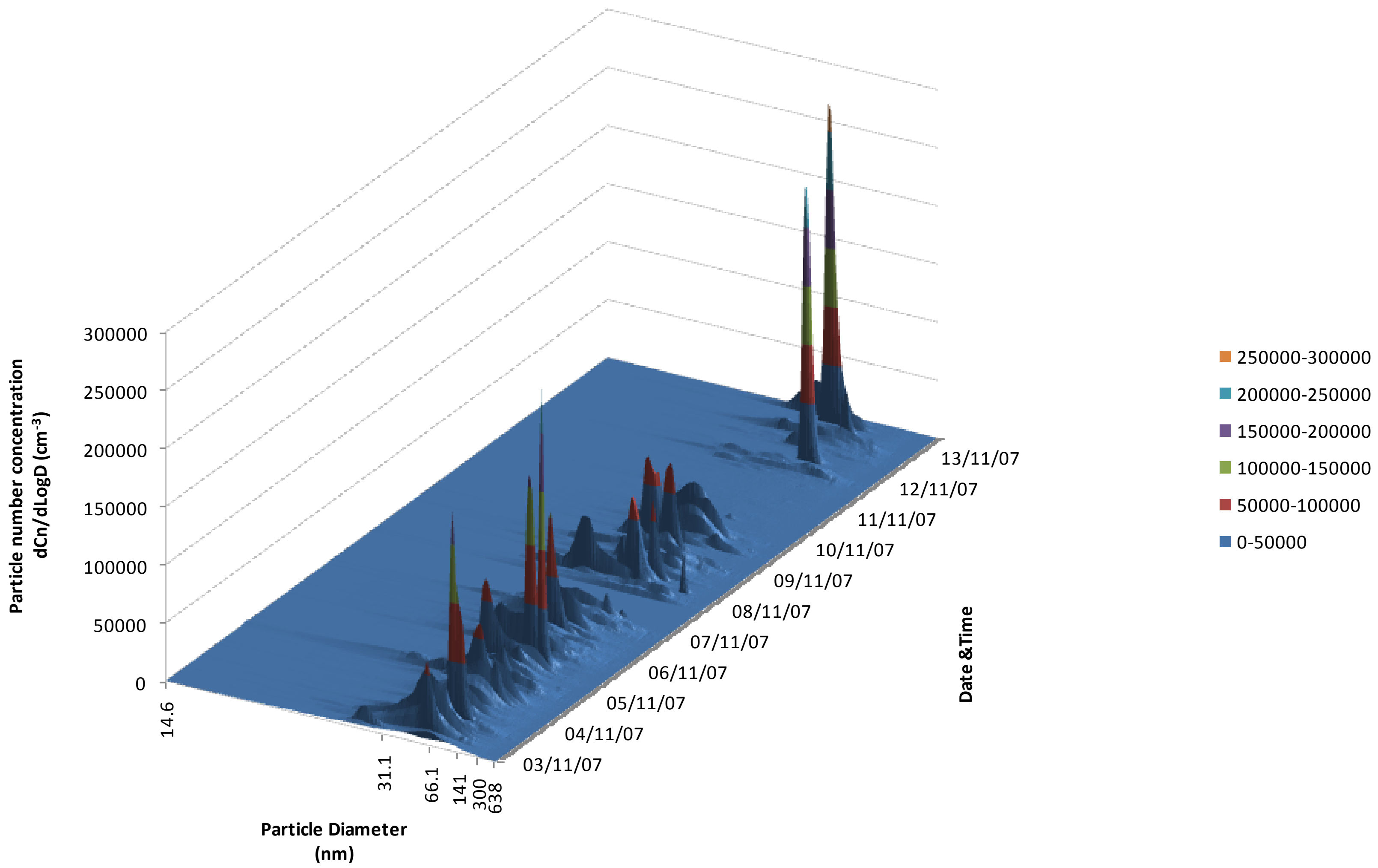

Figure 15: Particle number size distribution time series - Spring 2007

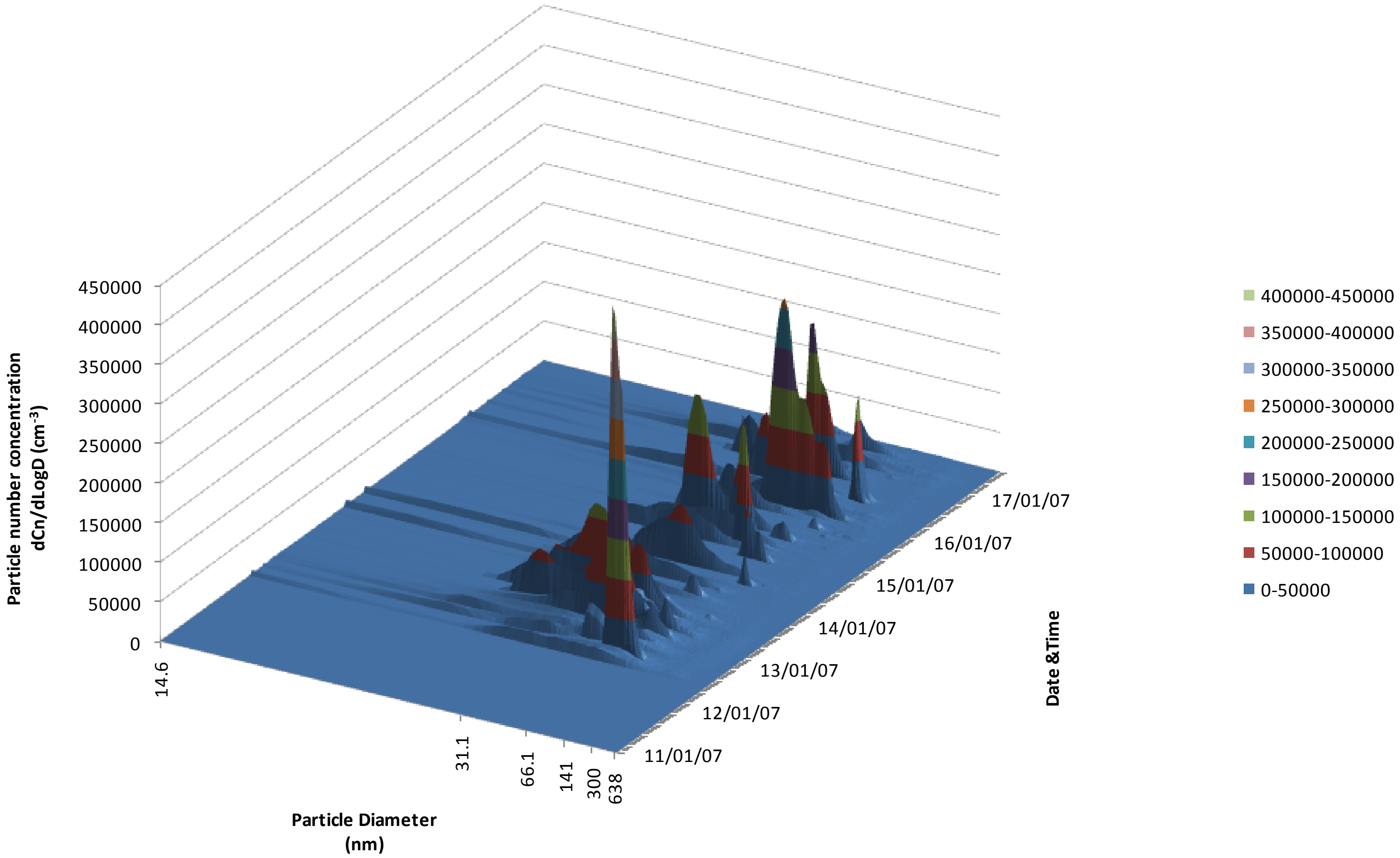

Figure 16: Particle number size distribution time series - Summer 2006-7

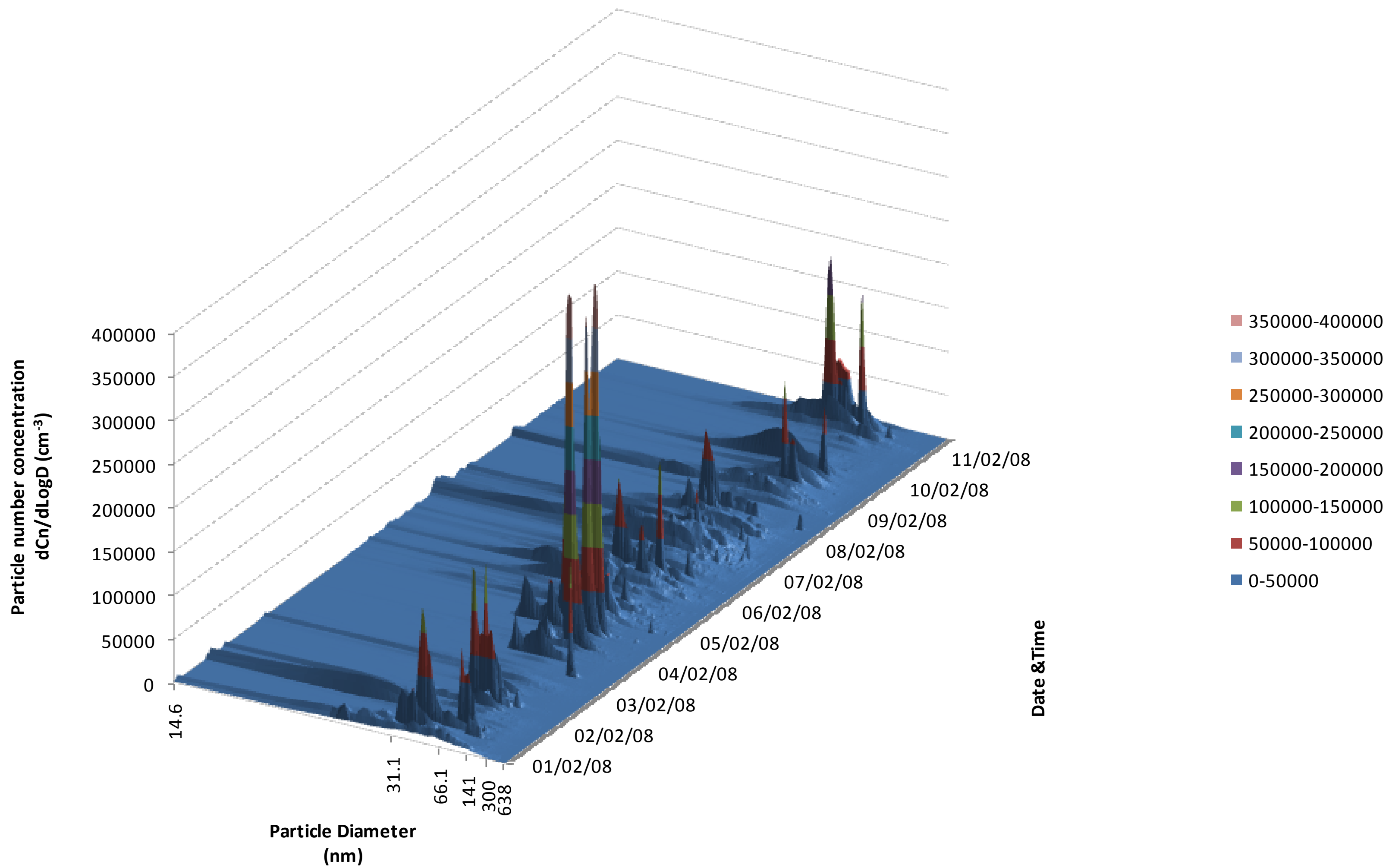

Figure 17: Particle number size distribution time series - Summer 2007-8

4.2 *Seasonal variations*

4.2.1 Seasonal average concentrations in successive years

Table 1 shows the average concentration for each campaign from Cn, $PM_{2.5}$, SO_2 and NO_2. The average values are also displayed in a bar graph in Figure 18. The prevailing wind direction during each campaign is shown in Figure 19. These are presented as polar plots of the total sampling time in the north, south, east and west quadrants for each campaign. Note that predominantly easterly winds as occurred in the spring 2007 campaign are expected to be associated with low concentrations due to the cleaner marine background overlaid by infrequent contributions from passing trains.

Table 2: Average concentration in each season for 2006 and 2007.

	Cn (x1000) (cm^{-3})		**$PM_{2.5}$ ($\mu g.m^{-3}$)**		**SO_2 (÷1000) (ppm)**		**NO_2 (÷1000) (ppm)**	
	Ave	**SD**	**Ave**	**SD**	**Ave**	**SD**	**Ave**	**SD**
Autumn 2006	6.0	5	13	8	2.5	3	13	8
Autumn 2007	6.7	6	14	10	2.5	3	12	9
Winter 2006	9.4	8	2	3	1.8	3	12	9
Winter 2007	7.7	8	12	8	1.7	3	9	9
Spring 2006	4.1	3	5	30	1.5	2	6	5
Spring 2007	4.8	5	4	4	0.6	2	3	7
Summer 2006/7	6.0	9	9	10	2.1	5	4	6
Summer 2007/8	6.0	8	13	9	2.1	3	5	6

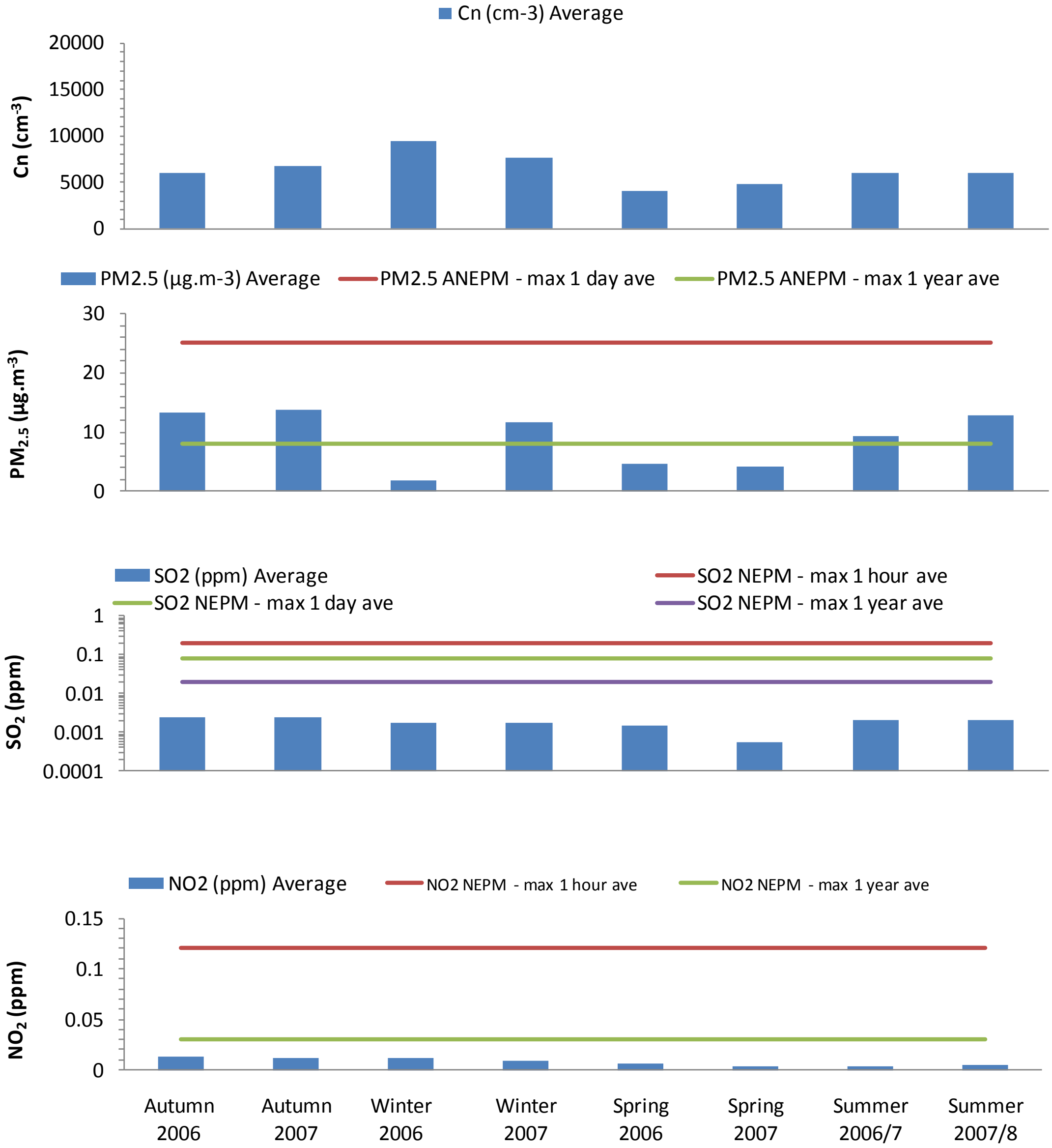

Figure 18: Bar graph of the average concentrations for each of the two week campaigns. Corresponding NEPM values are also shown where applicable.

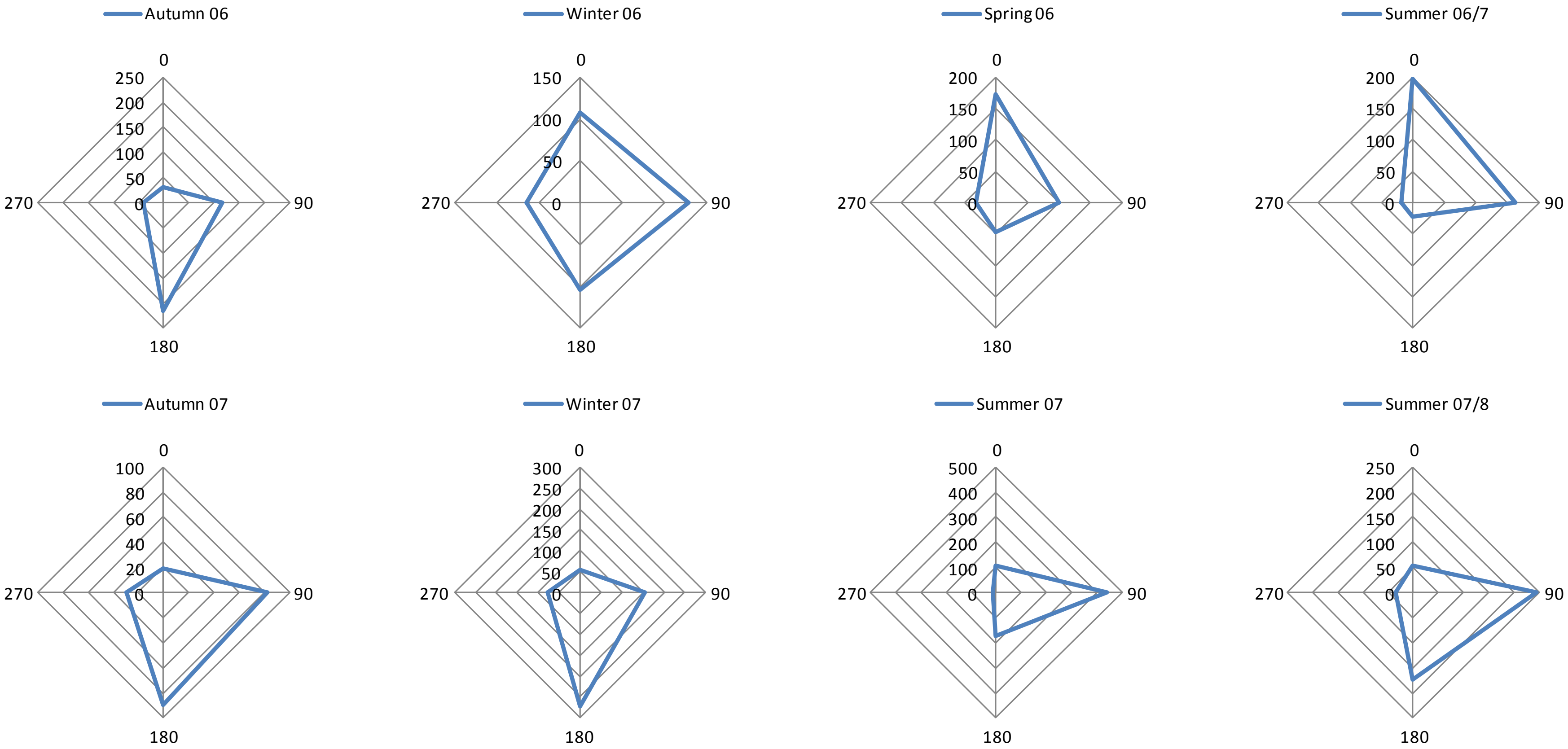

Figure 19: Total number of hours that wind was in each compass quadrant during sampling for each campaign.

4.2.2 Average seasonal particle number size distribution

Figure 20 shows the average particle number size distribution during each season combining the 2006 and 2007 campaigns. The size distribution appears to be dominated by diesel emissions in all cases as evidenced by the broad mode located at around 50 nm. The winter size distribution is slightly smaller in terms of modal diameter and is broader.

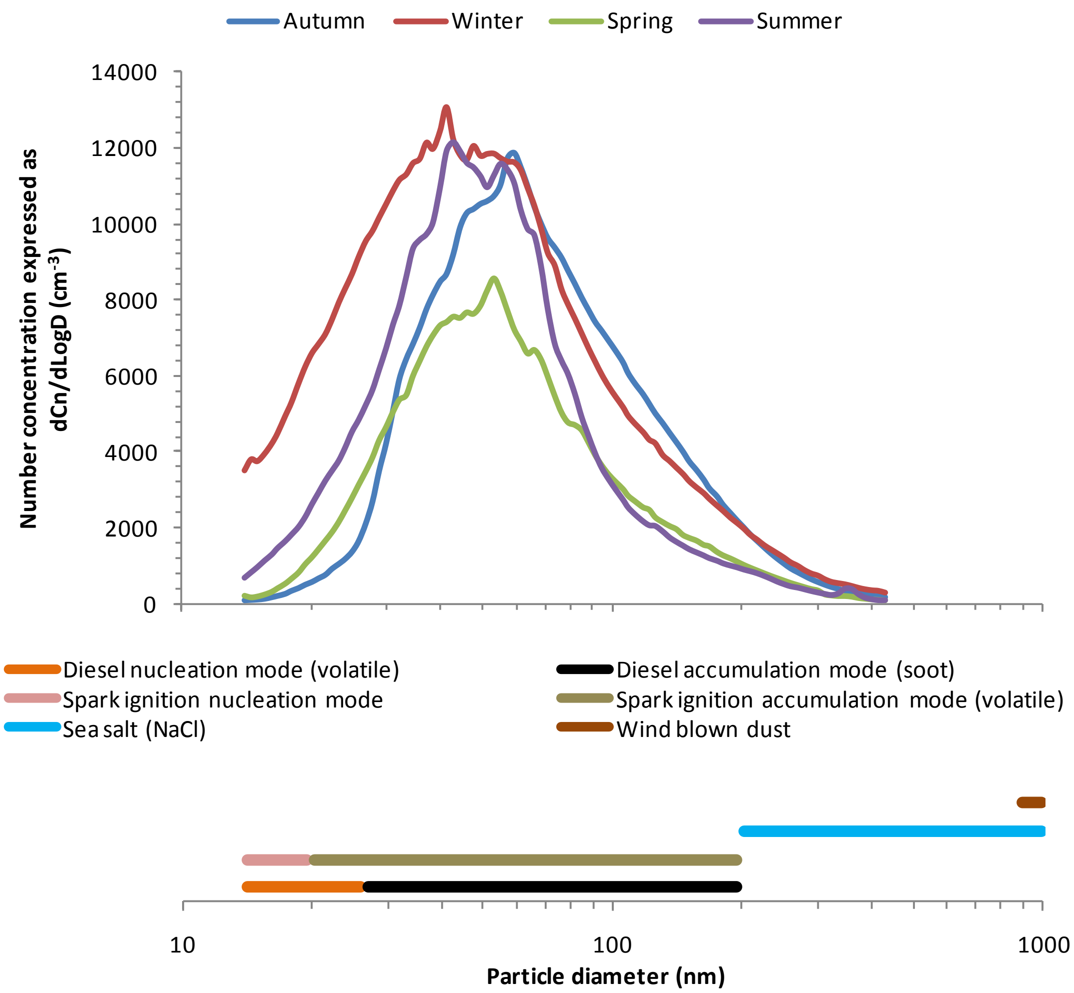

Figure 20: Average particle number size distribution in each season combining both years. Also shown are the expected sizes for particles from various sources.

4.3 Wind direction influence on concentration

4.3.1 Wind conditions during each two week measurement period

Figure 21 shows the average wind speed at the site with the long term average values measured at Brisbane Airport. Note that wind speed measurements depend strongly on the height above the surrounding terrain at which the monitoring is conducted. Substantially higher average values recorded at Brisbane airport may be due to higher elevation of the sensor.

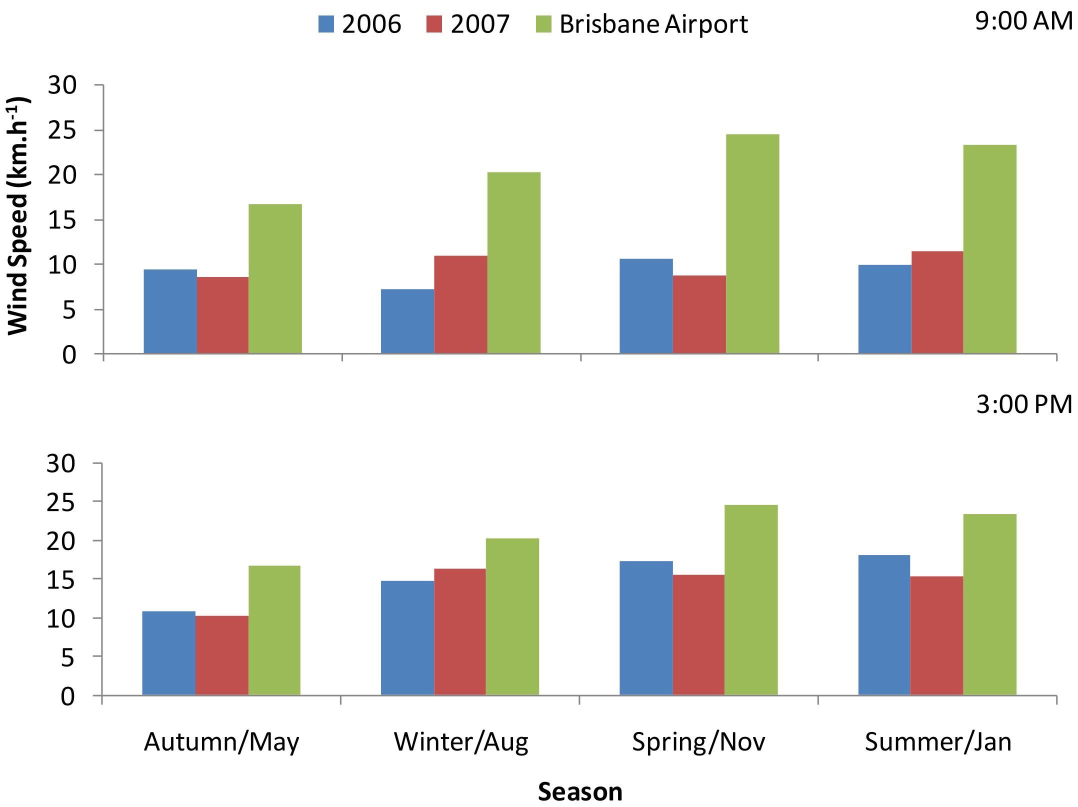

Figure 21: Average winds speed at 09:00 and at 15:00, at the monitoring site during each campaign and historical average at Brisbane Airport from 1994 to 2009.

Figure 22 shows the fraction of time the wind was at each compass point during each campaign at 09:00 and 15:00 as well as the corresponding historical long term average value recorded at Brisbane Airport.

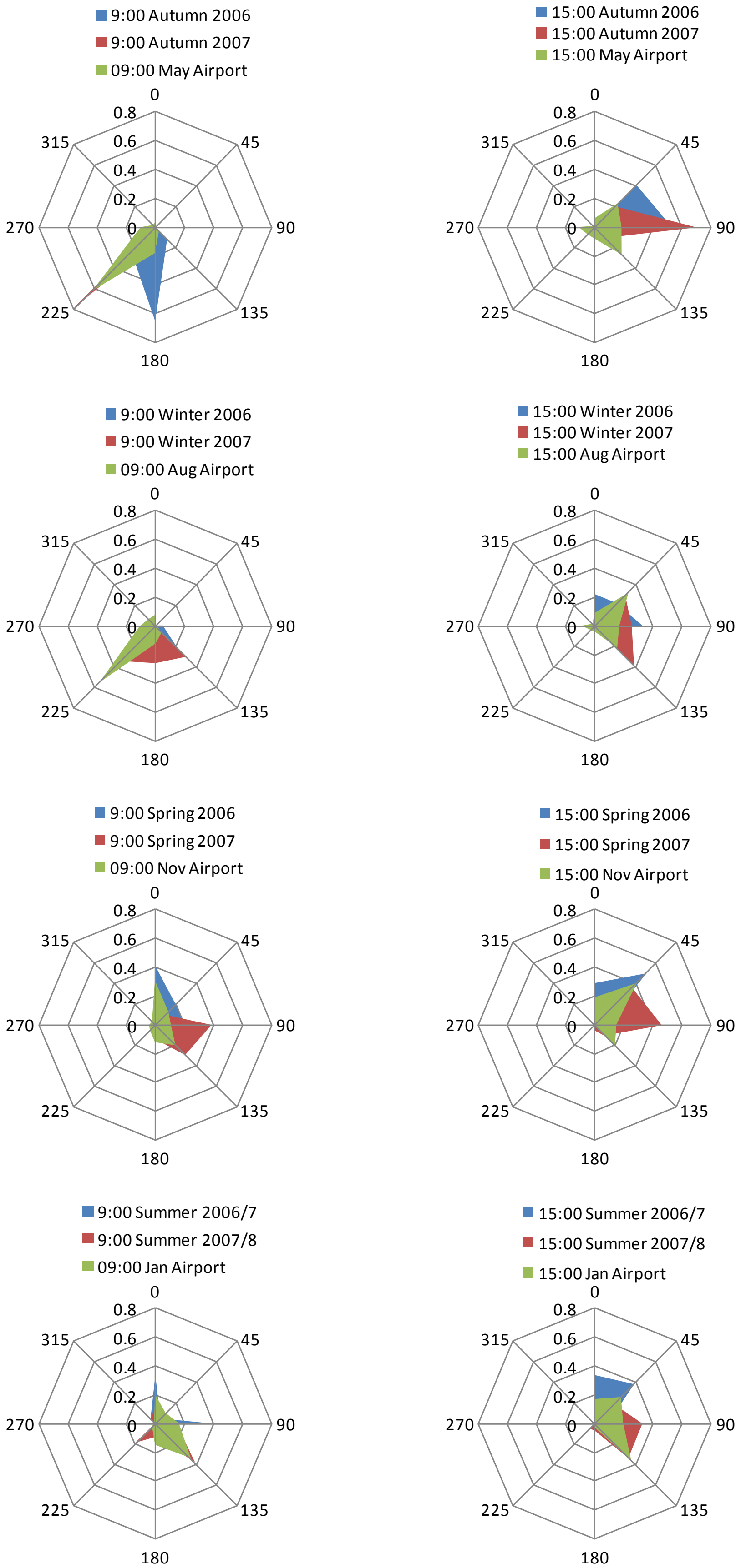

Figure 22: Comparison of time fraction in each compass sector at 09:00 and 15:00 for each campaign and long term average value at the airport weather station for the corresponding month and time.

4.3.2 Compass sector specific concentrations

In order to display the effect of wind direction on the concentration and size distributions, the data were classified according to wind direction into overlapping compass sectors, each 90 ° wide and centred on the points of the compass; North (N), Northeast (NE), East (E) and so on as defined in Table 3. Overlapping compass sectors were used in order to smooth out noise due to some having limited representation in the data set. The angular resolution in the data presentation is therefore 90º.

Table 3: Wind direction compass sectors

Compass Point	N	NE	E	SE	S	SW	W	NW
Bearing ±45 º	0 º	45 º	90 º	135 º	180 º	225 º	270 º	315 º

Polar plots of the average concentrations for each pollutant in each season are presented in Figure 23 and Figure 24. The average concentrations are recorded in Table 4.

Table 4: Average concentration in each compass sector (point) for each season.

	Summer	Autumn	Winter	Spring	All seasons
Compass Point	**Cn (cm^{-3}) (x1000)**				
N	8.4	5.9	9.4	5.1	7.2
NE	5.5	5.9	7.5	4.5	5.7
E	3.5	3.9	5.4	2.9	3.9
SE	4.2	3.4	5.6	3.4	4.3
S	7.6	7.2	9.0	5.2	7.6
SW	11	8.2	12	6.4	9.6
W	9.9	8.8	12	5.8	10
NW	8.2	7.8	11	4.4	7.8
	$PM_{2.5}$ ($\mu g.m^{-3}$)				
N	10	12	6.5	5.6	7.7
NE	9.6	10	5.2	4.0	6.8
E	8.3	9.4	4.9	2.2	5.9
SE	9.9	9.9	6.6	2.7	7.0
S	16	15	8.5	5.6	11
SW	21	16	9.9	8.3	13
W	20	18	11	10	14
NW	11	15	8.2	6.6	9.3
	SO_2 (ppm) (÷1000)				
N	2.4	1.8	3.1	1.8	2.3
NE	1.7	1.2	1.3	1.1	1.3
E	1.2	0.3	0.2	0.2	0.5
SE	1.2	0.9	0.4	0	0.5
S	3.2	3.8	2.1	0.7	2.4
SW	5.1	4.0	3.1	2.3	3.5
W	3.8	2.7	2.8	2.8	2.9
NW	3.8	2.3	3.4	2.7	3.1
	NO_2 (ppm) (÷1000)				
N	5.0	14	12	5.7	7.4
NE	2.7	10	7.2	4.9	5.0
E	1.7	5.0	3.3	3.7	3.0
SE	3.3	6.3	5.7	3.0	4.3
S	8.0	15	12	3.0	9.7
SW	11	17	17	4.1	14
W	11	21	19	6.5	16
NW	8.0	19	16	6.0	11

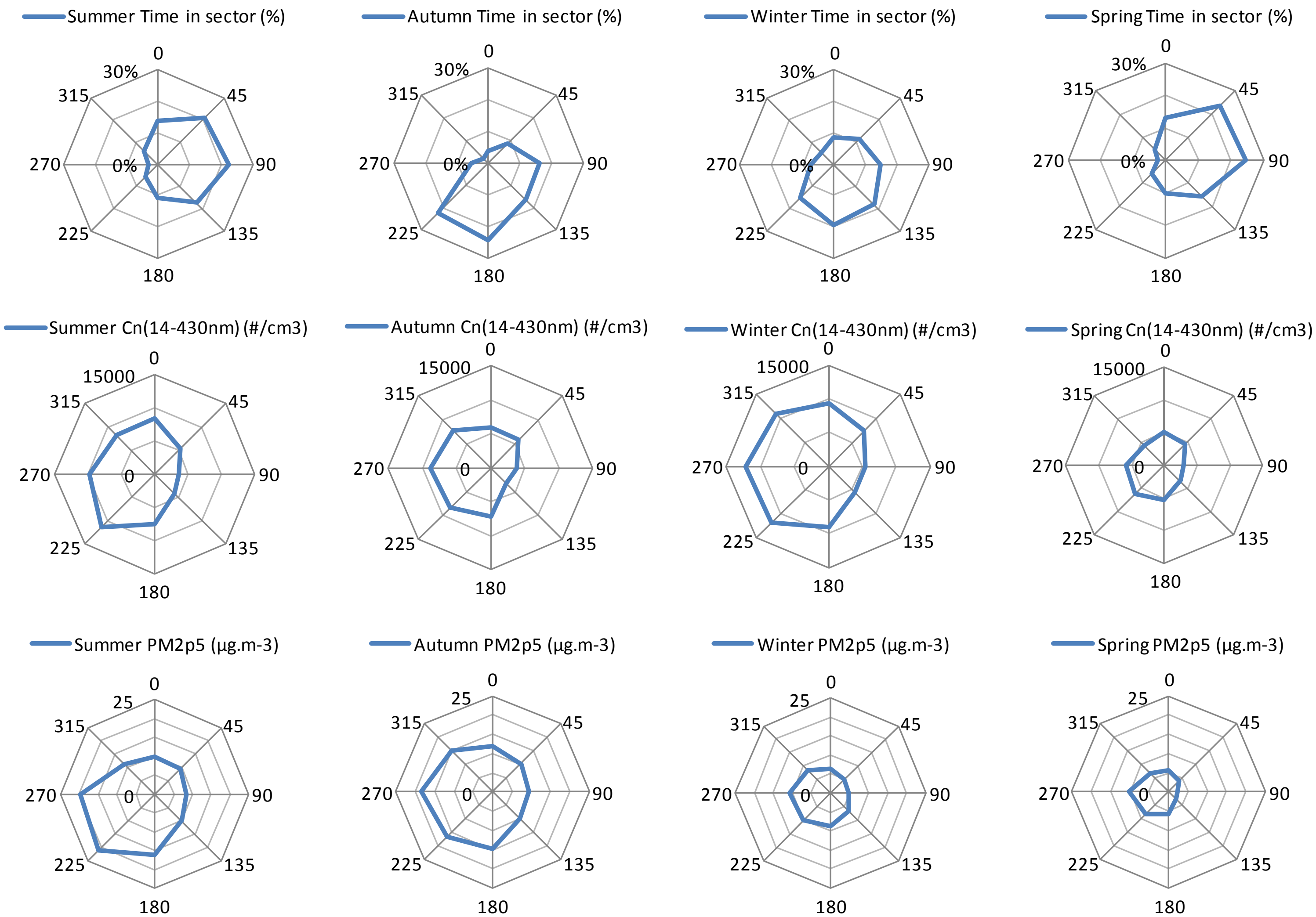

Figure 23: Fraction of time wind was in each compass sector, and the compass sector averages for Cn and $PM_{2.5}$ concentration.

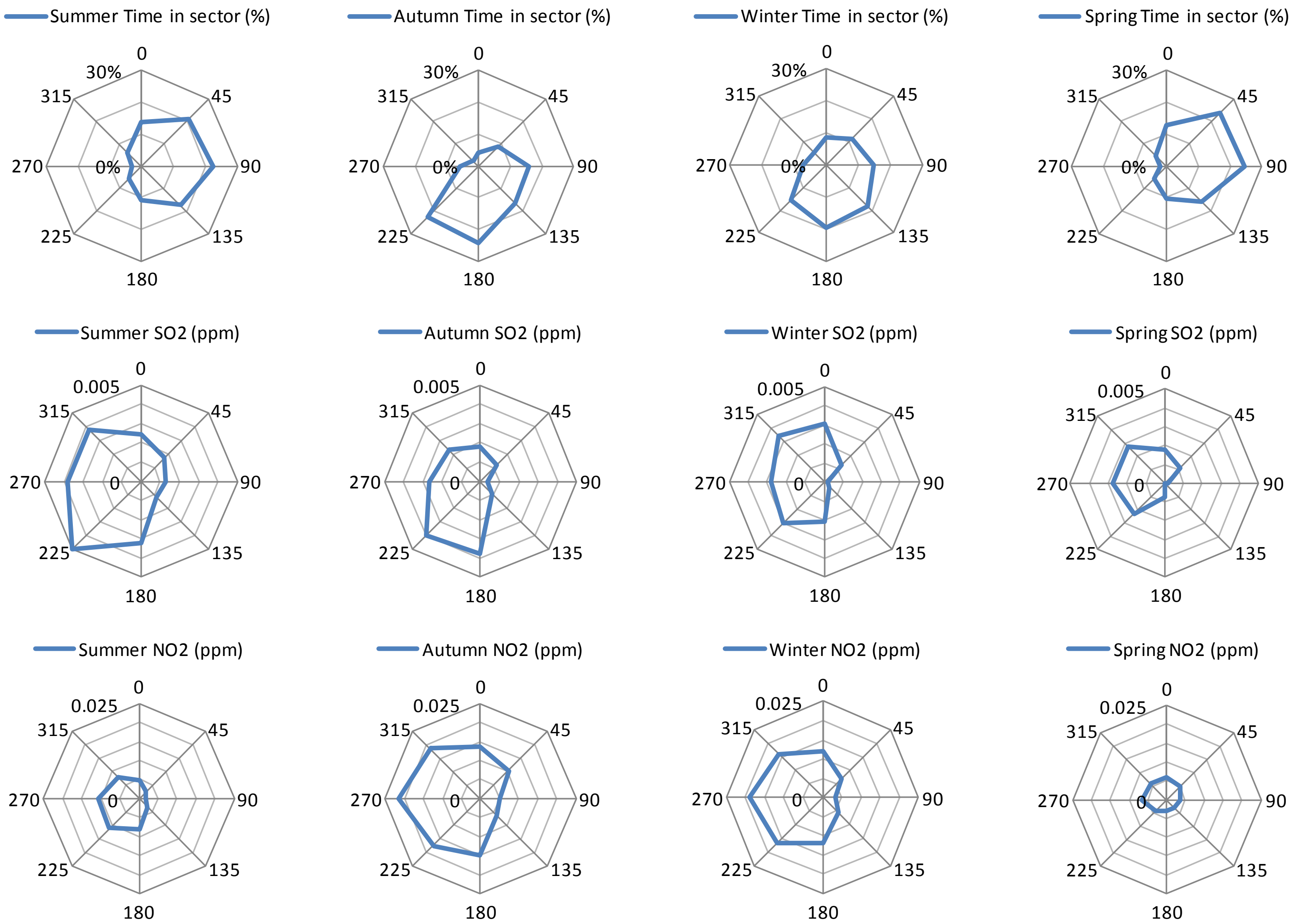

Figure 24: Fraction of time wind was in each compass sector, and the compass sector averages for SO_2 and NO_2 concentrations.

Some potential sources in each of the compass sectors are shown in Table 5. Based on these potential sources, four distinct source-sectors were identified. These are defined in Table 6 and illustrated in Figure 25. The source-sectors are labelled according to their characteristic influences.

Table 5: Compass sectors and associated potential sources.

Compass Point	Some Possible Sources
N	Port, Luggage Point
NE	Port, Marine
E	Rail, Marine
SE	Road, Urban, Marine
S	Road, Caltex Refinery
SW	Road, Caltex Refinery, BP Refinery
W	Road, BP Refinery, Luggage point, Airport
NW	Road, Luggage Point, Airport

Table 6: Definition of the source-sectors and their associated sources

Source-Sector Label	Bearing Range	Dominant influence in this source-sector
CA - Clean Air	45-135°	Marine environment
R - Residential	135-180°	Residential activities
LBI - Lower Brisbane Industrial	180-270°	Industry outside the port facility
PA - Port Activities	270-45°	Industrial areas of the port facility

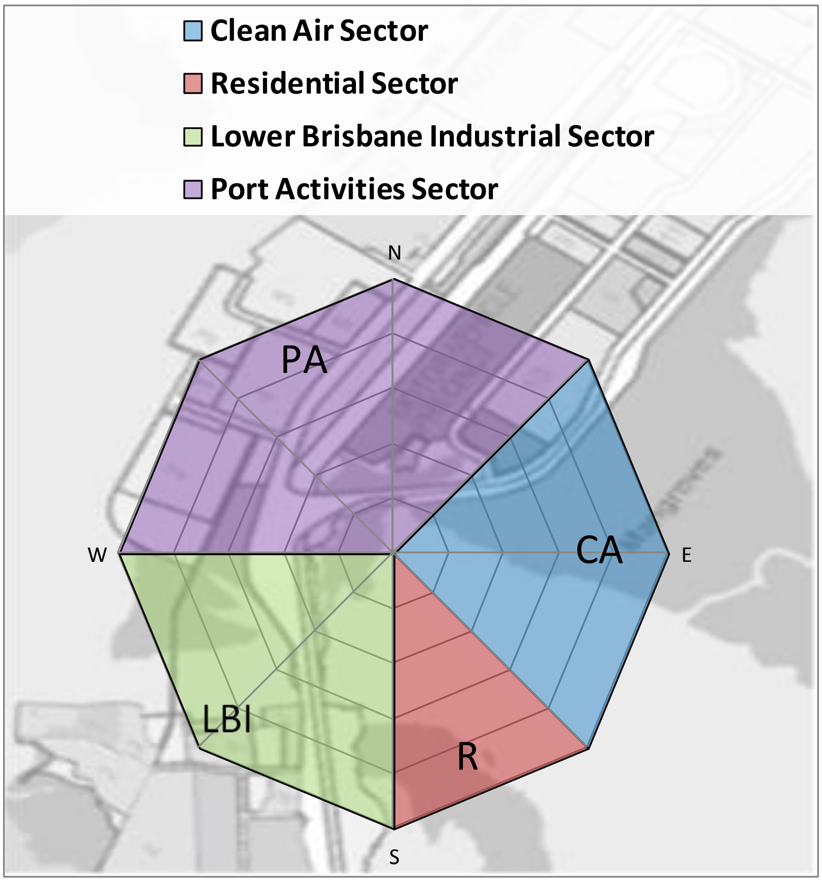

Figure 25: Source-sectors

Figure 26 shows the compass-sector average concentrations across all seasons for Cn, $PM_{2.5}$, SO_2 and NO_2 concentration. The source-sectors are also shown by colour shading as in Figure 25.

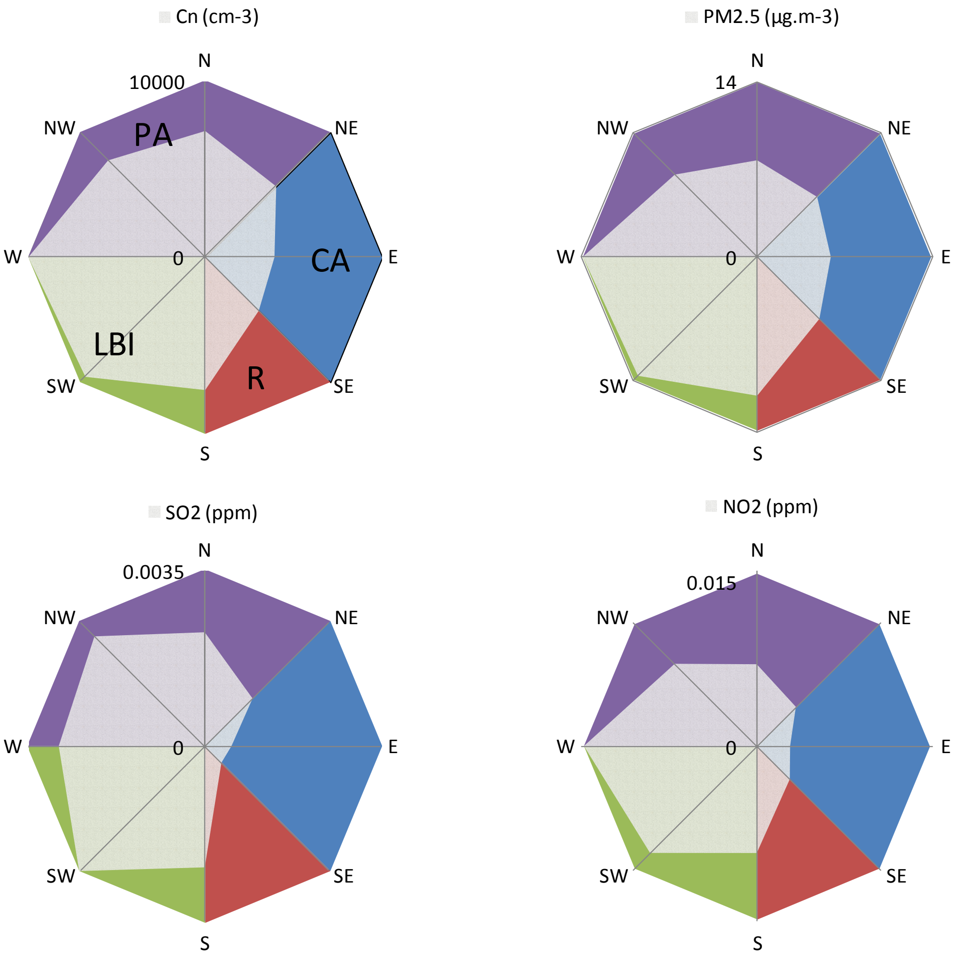

Figure 26: Compass sector averages across all seasons for Cn, $PM_{2.5}$, SO_2 and NO_2 concentration. Source-sectors are also shown, using colours as in Figure 25.

The $PM_{2.5}$ measurements do not target wind blown dust specifically. Dust is classified as either fine or coarse mode particulate matter, depending on the grain size. The fine and coarse mode particles are deposited at different rates. The coarse mode, with mass median aerodynamic diameters of about 5 to 6 μm deposits relatively quickly while the fine mode, $PM_{2.5}$, with mass median diameters below 2.5 μm, deposits much more slowly. This difference is due to the fact that larger particles have a higher gravitational settling velocity than small particles. The $PM_{2.5}$ deposition rates are roughly an order of magnitude lower than those for the coarse mode particulate matter. The fine/coarse ratio measured at downwind receptor sites can indicate the relative contribution of local versus distant sources of fugitive dust emissions. The scope of the current study did not permit such a detailed examination of dust concentrations however the study did include continuous measurements of $PM_{2.5}$ at the sample site over the period of each campaign.

$PM_{2.5}$ measurements detect the fine mode particulate matter which tends to be consistently transported over larger distances, even in light winds and is therefore more likely to be a persistent, as opposed to an occasional, nuisance at down wind receptor sites. As can be seen in Figure 23 and in Figure 26 there was no indication of a prominent source of fine particles in the PA source-sector. In fact more of this material appears to be associated with the LBI than the PA source-sector. It must be noted however that the road traffic common to both the LBI and PA source-sectors is in fact the dominant source in both.

For all pollutants measured, the concentration was highest in the LBI and PA source-sectors. In the case of SO_2 and to a lesser extent NO_2 the highest concentrations appear to be almost exclusively associated with the above two source-sectors. For Cn and $PM_{2.5}$ concentrations however, the CA and R source-sectors make significant contributions at the site. For all but the SO_2 concentrations, the strongest contribution on average came from the LBI source-sector while for SO_2 the concentrations associated PA and LBI source-sectors were similar.

These results suggest that the concentrations of NO_x, $PM_{2.5}$, SO_2 and Cn, measured in air which has passed over the port area (PA source-sector) are not significantly greater on average than in air which has passed over the LBI source-sector. The main source of all of these pollutants at the monitoring site appears to be the traffic on Port Drive.

4.3.3 Compass sector specific particle number size distribution

Figure 27 shows the average particle number size distribution for each compass sector and season combination averaged both study years.

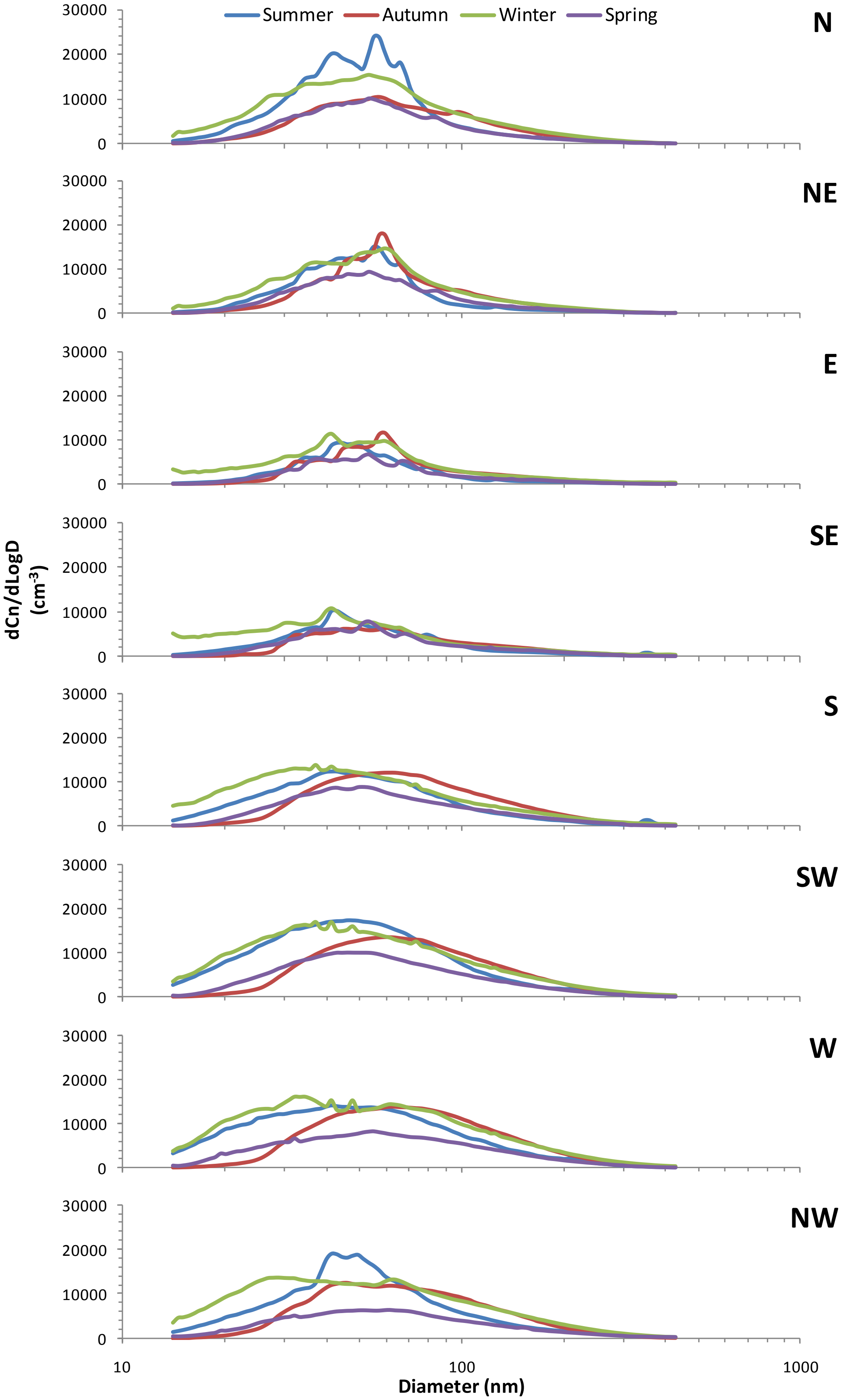

Figure 27: Particle number size distribution for each season for each compass sector averaged over both years of the study.

4.4 Relationship between traffic intensity and roadside concentration

Figure 28 through to Figure 32, show the relationship between the concentration and traffic intensity for each pollutant when the wind is blowing from the direction of the road. The values of R^2 are the square of the correlation coefficient; these represent the fraction of the concentration variance explained by the traffic intensity variation. Other factors likely to impact on the variance include the wind strength which tends to be higher during the day when traffic intensity also tends to be higher.

The linear trends shown on the graphs can be adopted as models for predicting roadside concentration on the basis of traffic intensity on the assumption that other factors such as wind speed also maintain their relationship to traffic intensity. Note that more sophisticated modelling may isolate the effects of traffic and wind speed but this is beyond the current scope of this project.

The linear trend model (concentration = slope x traffic + intercept) can be used to predict the one hour average concentration of the pollutant for a given level of traffic intensity (expressed as vehicles per hour), when the wind is from the direction of the road.

In the figures, model estimate of the fitting function is represented by the red line. The green lines represent the 95% confidence limits of the estimate of the true fitting function. The blue lines represent the bounds within which according to the model, a measurement of the one-hour average concentration will fall, 95% of the time.

The NEPM and ANEPM limits which have already been exceeded, or which might be expected to be exceeded as traffic intensity increases further in the future, are also shown.

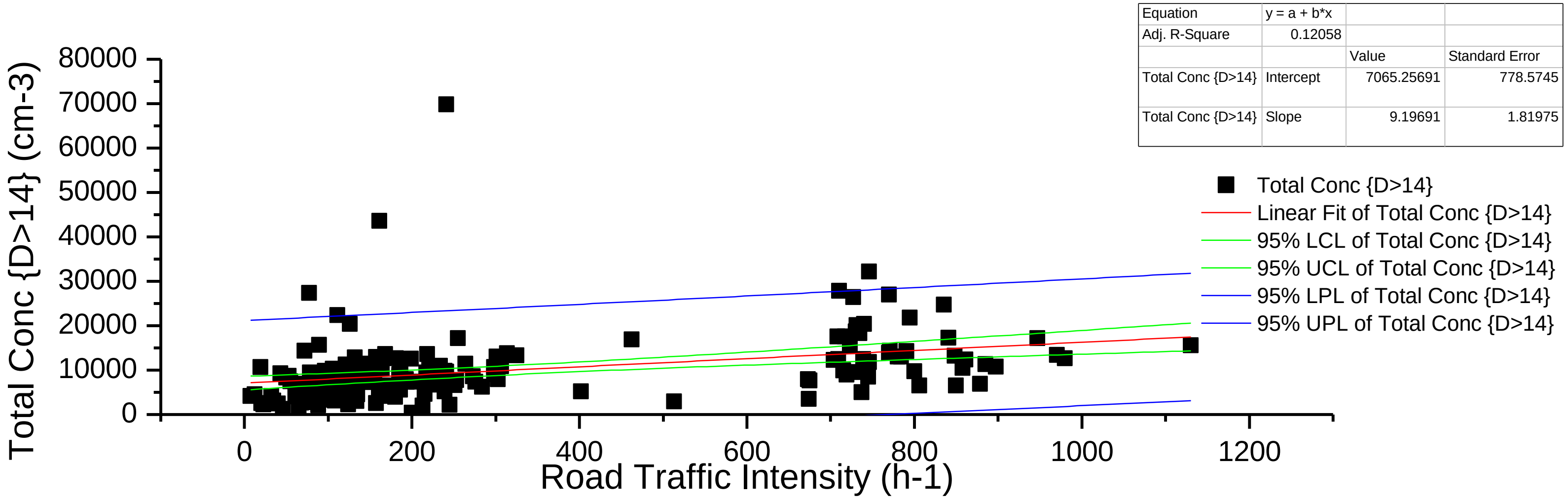

Figure 28: Relationship between Cn and road traffic intensity when winds come from the direction of the road. Also shown are the 95% confidence (LCL and UCL) and prediction (LPL and UCL) limits for the linear model.

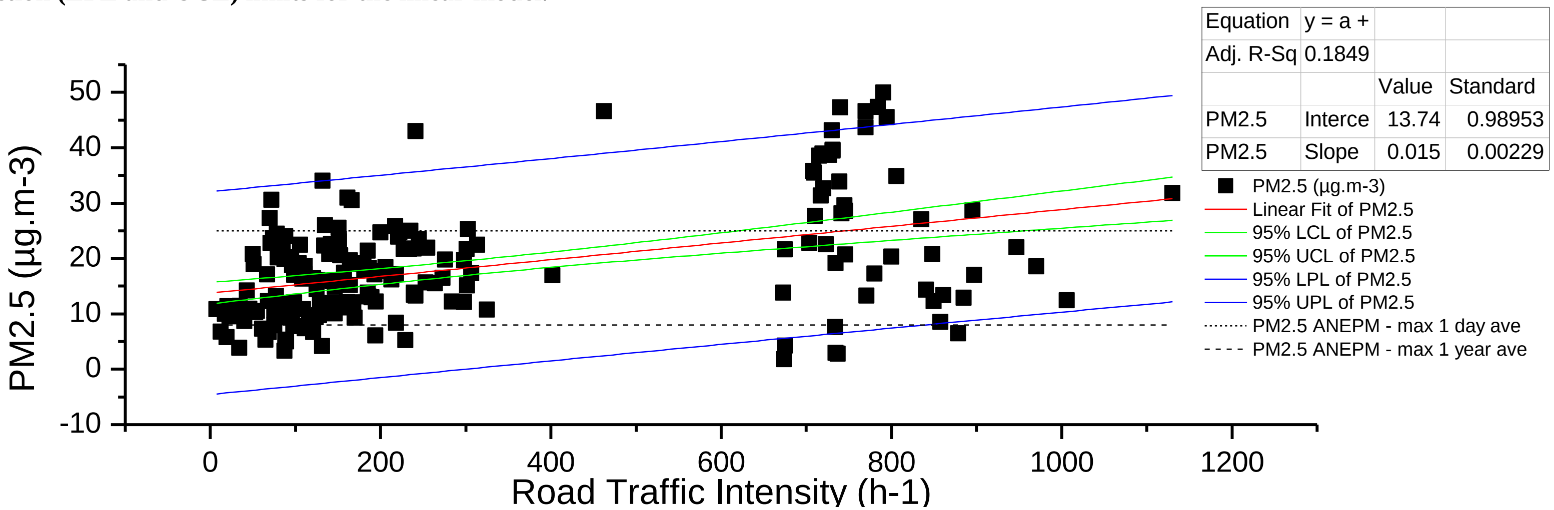

Figure 29: As above for $PM_{2.5}$ ANEPM 1 day and 1 year limits also shown.

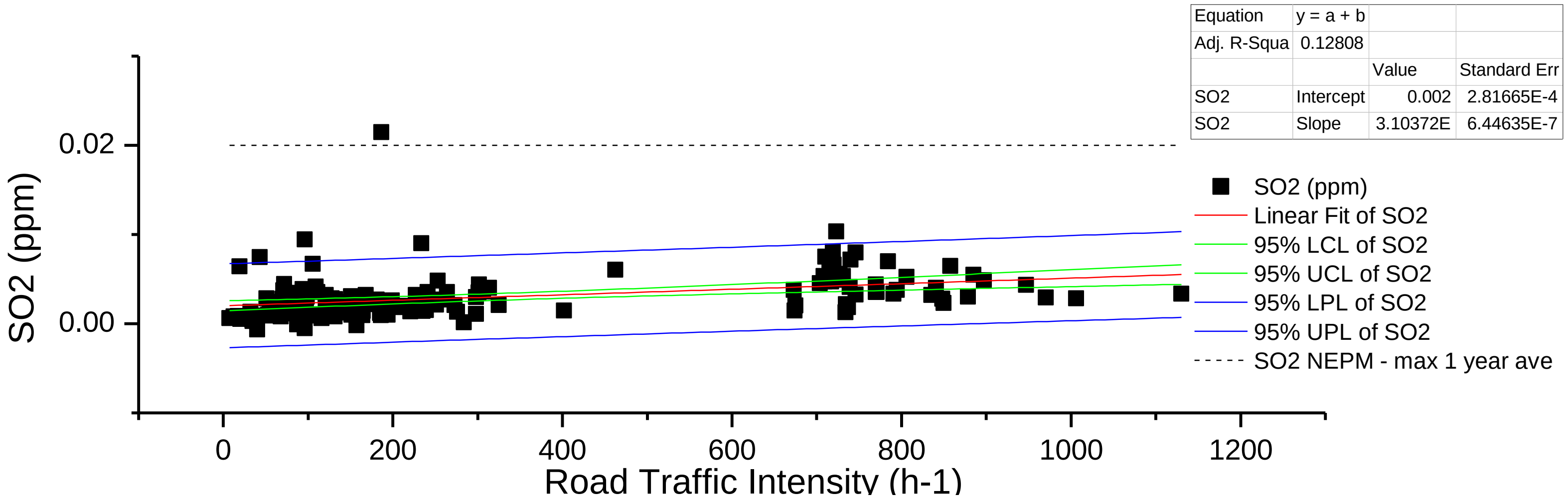

Figure 30: As above for SO_2. NEPM 1 year limit also shown.

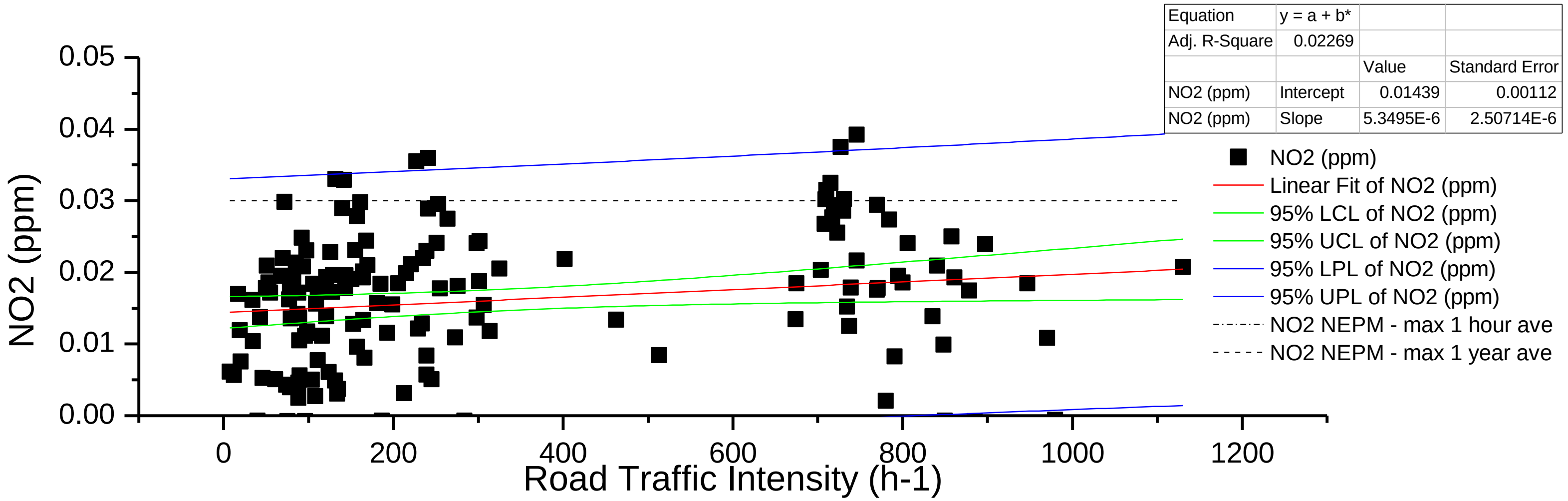

Figure 31: As above for NO_2. NEPM 1 hour and 1 year limits also shown.

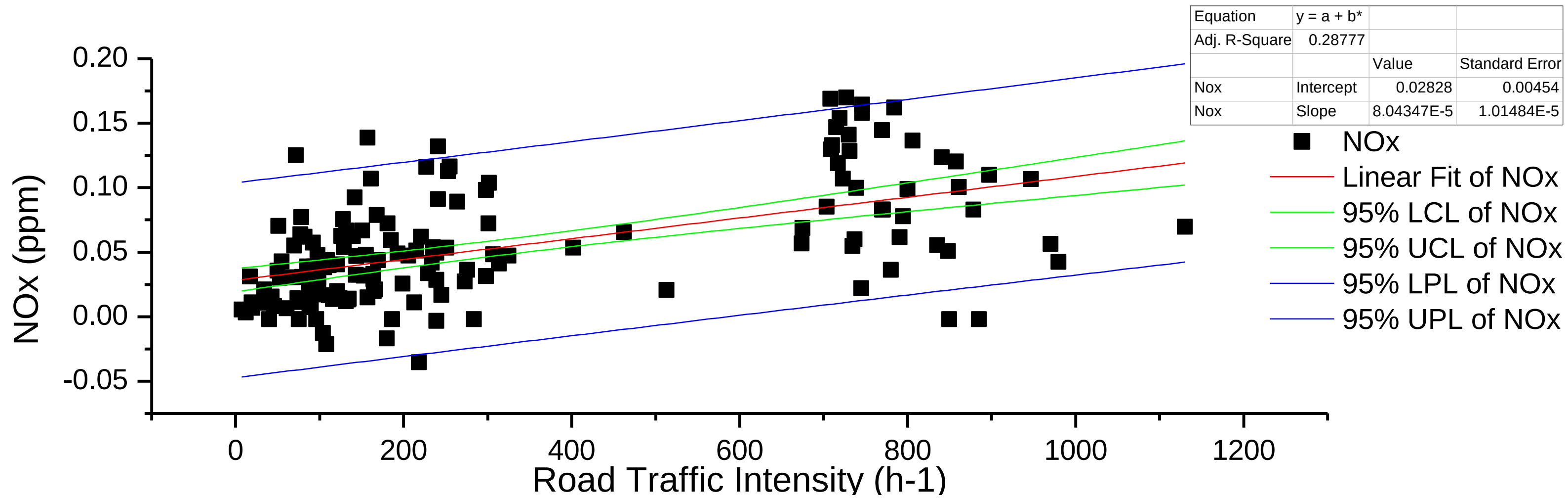

Figure 32: As above for NO_x

5 Summary

This report has presented an overview of the data collected in the Airborne Emissions- Port of Brisbane, Fisherman Islands Roadside Monitoring Study 2006-2008 during which airborne particulate and gaseous pollutant concentrations and meteorological conditions were measured in a series of eight seasonal campaigns spanning a 2 year period from January 2006 to February 2008. The monitoring was conducted from a trailer located between Port Drive, and the Railway line, at the southern tip of Fisherman Islands, immediately north of Captain Bishop Bridge.

This report included time series data for each of the eight campaigns including, campaign specific time series concentration data for each pollutant and campaign specific time series data for particle size distribution.

Seasonal variations including seasonal average concentrations of pollutants in successive years were presented as well as the average seasonal particle number size distributions.

The influence of wind direction on the concentrations and size distributions was presented by displaying compass sector specific concentration data and compass sector specific particle number size distributions

The relationship between traffic intensity and roadside concentration during periods when the wind carries traffic emissions from the road to the monitoring site was examined and a model of the relationship between traffic intensity and roadside concentration at the monitoring site was presented along with prediction limits and confidence limits for the model.

Morning and afternoon wind conditions during each two week measurement period were also shown in comparison to long term historical averages at the nearby Brisbane Airport weather station.

The analysis revealed a strong correlation between land use and pollutant concentrations. This correlation is evident in the strong relationships seen between wind direction and concentration. Four distinct source-sectors were identified:

- The Clean Air (CA) source-sector ranging from northeast through to southeast (45-135º) and influenced by the marine environment and Southern Moreton Bay Islands. This source-sector is also influenced by rail traffic emissions.
- The Residential (R) source-sector ranging from southeast through to the south (135-180º) taking in the residential community of Wynnum North and beyond. This source-sector also receives some influence from road traffic emissions from Port Drive.
- The Lower Brisbane Industrial (LBI) source-sector, ranging from south through to west (180-270º), taking in all of the Caltex and much of the BP oil refineries and strongly influenced by road traffic emissions from Port Drive.
- Port Activities (PA) source-sector ranging from west through to northeast (270-45 º), taking in the industrial areas of Port of Brisbane's Fisherman Islands complex and strongly influenced by road traffic emissions from Port

Drive and susceptible to influences from the BP Oil refinery, Luggage Point area and Brisbane Airport.

There was no indication of a prominent source of fine mode ($PM_{2.5}$) particles in the PA source-sector with more of this material associated with the LBI than the PA source-sector. Road traffic on Port Drive is common to both the LBI and PA source-sectors and is the dominant source in both of these source-sectors.

For all pollutants measured, the concentration was highest in the LBI and PA source-sectors. In the case of SO_2 and to a lesser extent NO_2 the highest concentrations appear to be almost exclusively associated with the above two source-sectors. For Cn and $PM_{2.5}$ concentrations however, the CA and R source-sectors make significant contributions at the site. For all but SO_2 concentration, the strongest contribution on average came from the LBI source-sector while for SO_2 the concentrations associated PA and LBI source-sectors were similar.

The concentrations of NO_x, $PM_{2.5}$, SO_2 and Cn measured in air which had passed over the port area (PA source-sector) were not significantly elevated in comparison to those measured in air which had passed over the LBI source-sector. The traffic on Port Drive was the dominant source of all of the pollutants measured at the monitoring site.

The information and analysis provided in this report represents a very significant improvement in our knowledge of airborne pollutants in the Fisherman Islands precinct. The report provides detailed information on airborne pollutant concentrations in the land transport access corridor for the Fisherman Islands precinct, which is a major local source of airborne pollutants. Hence the report provides an essential baseline against which future measurements can be assessed and from which predictions can be made concerning the impact of the future growth of the port and the resulting emissions in the precinct. By examining the relationships between airborne pollutant concentrations and port road traffic intensity it also provides a basis for predictions of future concentrations in the corridor as the intensity of transport activity changes.